

Systematic analyses identify modes of action of ten clinically relevant biocides and antibiotic antagonism in *Acinetobacter baumannii*

Received: 29 April 2019

Accepted: 11 August 2023

Published online: 9 October 2023

Liping Li^{1,2}, Francesca L. Short^{1,5}, Karl A. Hassan^{1,2,6}, Varsha Naidu^{1,2,6}, Alaska Pokhrel^{1,7}, Stephanie S. Nagy^{1,2}, Farzana T. Prity^{1,2}, Bhumika S. Shah^{1,2}, Nusrat Afrin^{1,2}, Stephen Baker³, Julian Parkhill^{1,4,8}, Amy K. Cain^{1,2}✉ & Ian T. Paulsen^{1,2}✉

 Check for updates

Concerns exist that widespread use of antiseptic or disinfectant biocides could contribute to the emergence and spread of multidrug-resistant bacteria. To investigate this, we performed transposon-directed insertion-site sequencing (TraDIS) on the multidrug-resistant pathogen, *Acinetobacter baumannii*, exposed to a panel of ten structurally diverse and clinically relevant biocides. Multiple gene targets encoding cell envelope or cytoplasmic proteins involved in processes including fatty acid biogenesis, multidrug efflux, the tricarboxylic acid cycle, cell respiration and cell division, were identified to have effects on bacterial fitness upon biocide exposure, suggesting that these compounds may have intracellular targets in addition to their known effects on the cell envelope. As cell respiration genes are required for *A. baumannii* fitness in biocides, we confirmed that sub-inhibitory concentrations of the biocides that dissipate membrane potential can promote *A. baumannii* tolerance to antibiotics that act intracellularly. Our results support the concern that residual biocides might promote antibiotic resistance in pathogenic bacteria.

Multiple-drug resistance (MDR) in bacterial pathogens is an alarming public health issue¹. Bacteria can resist drugs by expressing efflux pumps to export drugs out of the cell, altering outer membrane permeability to reduce drug accumulation, or expressing enzymes for drug

inactivation by hydrolysis or modification². Alternatively, bacteria can gain intrinsic resistance mutations that prevent target recognition or cause target bypass. The Gram-negative opportunistic human pathogen *A. baumannii* is a health threat for immunocompromised patients who

¹ARC Centre of Excellence in Synthetic Biology, Macquarie University, Sydney, New South Wales, Australia. ²School of Natural Sciences, Macquarie University, Sydney, New South Wales, Australia. ³Cambridge Institute of Therapeutic Immunology and Infectious Disease (CITIID), University of Cambridge, Cambridge, UK. ⁴The Wellcome Sanger Institute, Wellcome Genome Campus, Hinxton, Cambridge, UK. ⁵Present address: Infection Program and Department of Microbiology, Biomedicine Discovery Institute, Monash University, Clayton, Victoria, Australia. ⁶Present address: School of Environmental and Life Sciences, University of Newcastle, Callaghan, New South Wales, Australia. ⁷Present address: Australian Institute for Microbiology and Infection (AIMI), University of Technology, Sydney, New South Wales, Australia. ⁸Present address: Department of Veterinary Medicine, University of Cambridge, Cambridge, UK. ✉e-mail: amy.cain@mq.edu.au; ian.paulsen@mq.edu.au

are hospitalized in Intensive Care Unit (ICU) wards. This is due to the emergence of *A. baumannii* clonal lineages with high-level resistance to antimicrobials and tolerance to desiccation^{3,4}.

Biocides are disinfectants and antiseptics that are widely used for disinfection and cleaning in both households and hospitals, but little is known about their impact on the emergence and spread of MDR infections. In contrast to antibiotics, the use of biocides is largely unregulated. The recommended in-use biocide concentrations are normally orders of magnitude higher than the bacterial minimum bactericidal concentration. Biocides are presumed to have multiple antibacterial targets or non-specific targets, reducing the likelihood of bacteria developing resistance to these compounds⁵. There is evidence suggesting that biocide exposure at sublethal concentrations can select for antibiotic-resistant bacteria under laboratory conditions⁶, and clinical antibiotic-resistant isolates typically have reduced biocide susceptibilities⁷. One of the most commonly known biocide and antibiotic cross-resistance mechanism is the activity of MDR efflux pumps, such as AcrAB-TolC from *Escherichia coli*⁸ and AdeIJK and AdeABC from *Acinetobacter baumannii*⁹.

Biocide modes of action are generally poorly characterized, except for cell lysis via interaction with the phospholipid membrane⁵. However, some biocides are known to have a mode of action that start intracellularly. For example, silver ions can interact with the thiol group of exposed cysteine residues leading to enzyme inactivation and disruption of cellular iron homoeostasis^{10,11}, and they also cause cell membrane proton leakage¹². The known silver resistance determinants are primarily involved in reducing silver ion intracellular concentration, including membrane transporters for silver ion export¹³ and proteins for neutralization or reduction of silver ions to the inactive metallic form¹⁴. Triclosan targets an intracellular essential enzyme enoyl reductase (FabI) in fatty acid synthesis¹⁵. Key determinants for high-level triclosan resistance include MDR efflux pumps and either mutations in the *fabI* gene or the acquisition of alternative Fab proteins not recognizable by triclosan¹⁶. Apart from the drug efflux pumps mentioned earlier, members from the proteobacterial antimicrobial compound efflux (PACE) family confer resistance to antibacterial surfactant compounds including chlorhexidine and benzalkonium¹⁷. These observations suggest that the surfactant biocides are also likely to have intracellular targets, or these pumps can expel them from the membrane.

Knowledge of both biocide modes of action and tolerance mechanisms is important for improved biocide use for effective and sustainable infection control. Here we performed a systematic genome-wide screen to identify genes that affect susceptibilities of an MDR *A. baumannii* strain to ten clinically important biocides (Extended Data Table 1) using transposon-directed insertion-site sequencing (TraDIS)^{18,19}.

Results

TraDIS experimental outcomes

TraDIS assays were performed on a global clone II multidrug-resistant *A. baumannii* strain BAL062 transposon mutant library²⁰ to assess the global genetic response to biocide treatments. Ten structurally distinct biocides were chosen for this study; these are all either listed as ‘essential medicines’ by the WHO or are commonly used in clinical settings and/or as household products (Extended Data Table 1). The *A. baumannii* TraDIS library was exposed to a sub-inhibitory concentration of each biocide (Extended Data Table 2) and TraDIS analysis was performed²¹. Gene-wise mutant abundance data were compared to untreated control samples grown under identical conditions to identify mutations that affect fitness in the presence of biocides. Collectively, the biocide treatments revealed a range of genes harbouring a reduced mutant population (that is, decreased insertion read counts; 3–120 genes), representing potential biocide tolerance determinants, or an expanded mutant population (that is, increased insertion read counts;

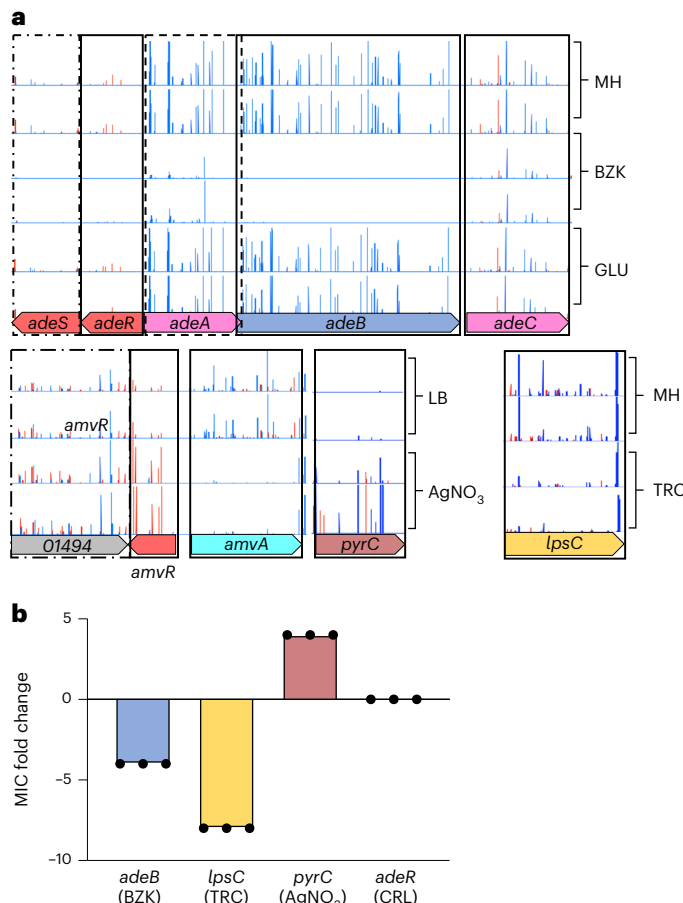


Fig. 1 | Biocide TraDIS data. **a**, Representative genes and TraDIS insertion plots. Coloured horizontal arrows represent gene length and direction, with gene names indicated therein. Above each gene are lines representing reads mapped from each Tn5 insertion site, with height of the line representing the number of reads. The black box height represents a maximum of 100 reads in all conditions, except *lpsC* with 10 reads. For each condition, two biological replicates of TraDIS results are presented. The dashed and dashed-dotted boxes are for visualization of the transposon insertion reads for each gene cassette. The arrow colours correlate with the MIC results in **b**. **b**, MIC fold change of four different mutants for relevant biocide compounds compared with the ABS075 wild-type strain, including three biological replicates for each condition. Data are presented mean \pm s.d. Biocides are listed as abbreviations (see Extended Data Table 1). The data were processed and plotted using GraphPad Prism v.10.0.0 (131).

7–100 genes) whose inactivation is potentially beneficial under biocide treatment (Extended Data Table 1).

We examined genes previously associated with biocide resistance and found their functions reflected in the TraDIS results. For example, the MDR efflux pump-encoding operon *adeABC* and its activator genes (*adeRS*) showed significantly decreased insertion read counts (for example, *adeB* had a 115.4-fold decrease) after treatment with benzalkonium, a known substrate of AdeABC, whereas no change was seen after treatment with glutaraldehyde, which is not known to be a substrate of AdeABC (Fig. 1a).

Genes previously associated with antibiotic resistance were identified: for example, *lpsC*, a glycosyltransferase and LOS (lipooligosaccharides) synthesis gene involved in polymyxin resistance in *A. baumannii*²² but not previously implicated in biocide resistance, showed a 5.8-fold decrease in insertions following triclosan treatment (Fig. 1a). We also revealed potential new roles in biocide resistance for previously characterized genes: for example, the insertions in the pyrimidinesynthesis gene *pyrC*²³ showed a 35.9-fold increase in AgNO₃-treated cultures compared with the control (Fig. 1a).

As proof-of-principle phenotypic validation of this TraDIS data, we measured the minimum inhibitory concentration (MIC) or growth curves for all ten biocides on 13 isogenic single-gene knockout Tn26 mutants from *A. baumannii* AB5075 24 (Extended Data Table 3). These include *trpA* (tryptophan synthase subunit alpha), *gltA* (citrate synthase), BAL062_00464 (ribonuclease I), *adeF* (MDR efflux pump), BAL062_00031 (putative drug efflux pump), *amvA* (MDR efflux pump), *lysA* (diaminopimelate decarboxylase), *dsbA* (thiol:disulfide interchange protein), *rvB* (Holliday junction DNA helicase) and the genes outlined above: *adeB*, *lpsC*, *pyrC* and *adeR*. For *adeB*, *lpsC*, *pyrC* and *adeR*, the biocide MIC fold change for the mutant relative to wild type was essentially consistent with the TraDIS results (Fig. 1b).

The TraDIS data reflect subtle population dynamic changes, which is probably more sensitive than standard MIC assays. For the remaining nine genes, we additionally performed growth curve assays. The growth curve differences between the mutants and the parental strain are essentially consistent with the TraDIS data (Extended Data Figs. 1 and 2, and Table 3). For both the MIC and growth curve data, polyvidone iodine is the one compound that was not consistent with the TraDIS data, as we observed no changes in susceptibility to this compound in the mutants tested here. To ensure that the phenotypes that we observed on these isogenic single-gene knockout transposon mutants were not derived from secondary mutations, we tested five representative genes for further growth curve assays using a second, independent transposon mutant of the same gene. We showed that the two transposon mutant pairs of each of these five genes share similar biocide tolerance phenotypes (Extended Data Fig. 2).

Outer membrane lipooligosaccharide

A. baumannii lacks a homologue of the O-antigen ligase WaaL, which transfers O-antigen polysaccharide onto the outer core of lipopolysaccharides, suggesting that *A. baumannii* lipopolysaccharides may comprise only lipid A and core oligosaccharide²⁴. We observed that insertions in a lauroyl acyltransferase-encoding gene, *lpxL*, increased following treatment with the cationic surfactants chlorhexidine and cetyltrimethylammonium bromide (CTAB) (21- and 2.3-fold, respectively), suggesting that this gene decreased fitness to these two biocides (Fig. 2a). The predominant glycolipid molecule in the outer leaflet of *A. baumannii* outer membrane is hepta-acylated lipid A²⁵, whereas an *lpxL* mutant generates a hexa-acylated lipid A²⁶. This change in fatty acid profile may impact the effectiveness of these biocides against *A. baumannii*.

Cell surface polysaccharides

In *A. baumannii*, there are two gene clusters known to be involved in capsule polysaccharide biosynthesis (K-locus) and LOS outer core oligosaccharide biosynthesis (OC-locus)²⁷. We identified 9 genes in the K-locus with significant changes in insertion counts after treatment with one or more biocides. For instance, insertions in the *gna* gene, encoding a UDP-glucose dehydrogenase, increased during treatment with chlorhexidine and bleach (207- and 3.2-fold, respectively), implicating capsule polysaccharide in biocide sensitivity.

Insertions in a glycosyltransferase-encoding gene, *pglC*, had decreased read coverage (9.9-fold) when treated with AgNO₃, while treatment with the other 9 compounds did not have an effect, suggesting that this gene may mediate tolerance only for AgNO₃ (Fig. 2a). *pglC* is located in the variable region of the K-locus, but its presence is conserved in this gene cluster across *A. baumannii* strains^{27,28}. It is required for the construction of capsular glycan repeat units and glycosylation of glycoproteins²⁸, and the deletion mutant affects capsule production but not LOS²⁹. In addition to *pglC*, insertions in 7 other genes in the K-locus also displayed decreased frequency following AgNO₃ treatment (Fig. 2a), implying that the capsular polysaccharide may play a specific role in AgNO₃ tolerance, whereas alteration of LOS glycoforms impacts susceptibility to biocides more broadly.

Insertions in 7 genes in the OC-locus had altered frequency following biocide treatment (Fig. 2a). For instance, insertions in the glycosyltransferase gene *lpsC* decreased 5.8-fold following exposure to benzalkonium. Further, insertions in another glycosyltransferase gene, *gtrOC3*, dropped dramatically (78.8-fold) upon chlorhexidine treatment (Fig. 2a). Insertions in the glycosyltransferase gene *lpsB*, which is outside of the two polysaccharide biosynthesis loci and is involved in LOS core biosynthesis, also showed changes following exposure to 7 biocides (Fig. 2a). Previously, it has been shown that disruption of these glycosyltransferases in *A. baumannii* produces truncated LOS^{30,31}. Thus, genes predicted to encode glycosyltransferases, which catalyse the linking of sugars of the LOS outer oligosaccharide core, may be important in biocide tolerance.

Chaperone-usher pilus

Another potential cell surface biocide tolerance determinant identified in this study is a chaperone-usher pilus gene cluster *csuA/BABCDE* (Fig. 2a)³², insertions in which decreased after treatment with 8 biocides (Fig. 2a). Insertions in all the *csu* genes decreased with most biocides (Fig. 2a). Consistent with their known function as *csu* operon activators, insertions in the 2-component system genes *bfnRS* also decreased following treatments with 7 out of the same 8 biocides (Fig. 2a). Insertions in a transcriptional regulator (BAL062_01328) directly upstream of the *csu* operon also decreased in frequency following treatment with the same 8 biocides and the fold change was similar to that of *csu* gene mutants (Fig. 2a), indicating that BAL062_01328 encodes a potential local transcriptional activator of the *csu* operon. Together, these results suggest that the mature pilus system is required for a biocide tolerance phenotype.

Membrane transport

Sixteen drug efflux systems have been characterized or identified in *A. baumannii*³³. One of the most clinically relevant drug transporters in *A. baumannii* is a tripartite efflux system AdeABC³⁴, comprising a membrane fusion protein (MFP) AdeA, a resistance-nodulation-division (RND) efflux pump AdeB and an outer membrane factor (OMF) AdeC. This system is constitutively overexpressed in clinical *A. baumannii* MDR strains, typically due to mutations in the 2-component transcriptional activator genes *adeRS*³⁵.

Transposon mutants of *adeB* decreased following treatment with benzalkonium, cetrimonium, chlorhexidine, triclosan and chloroxylenol (Fig. 2b), suggesting that *adeB* mediates resistance to these compounds. Benzalkonium and chlorhexidine are known AdeB substrates⁹. Surprisingly, Tn5 insertion changes in *adeA* and *adeC* were only seen with benzalkonium and chlorhexidine (Fig. 2b), where both were decreased (Fig. 2b). This suggests that AdeABC functions as a tripartite system to pump out these two compounds.

Insertion decreases in *adeR* and *adeS* were seen in benzalkonium and chlorhexidine mutant pools, whereas no change was observed in the other three conditions that also selected against *adeB* mutants (Fig. 2b). A transcriptomics study showed that chlorhexidine can induce the expression of *adeABC* in *A. baumannii* ATCC17978 (ref. 36). Using RT-qPCR (reverse transcription quantitative polymerase chain reaction), we showed that benzalkonium and chlorhexidine can induce higher levels of *adeB* transcription in *A. baumannii* BAL062 (Fig. 2c). The transposon mutant of *adeB* in *A. baumannii* AB5075 is more sensitive to benzalkonium, chlorhexidine, triclosan, CTAB and chloroxylenol (Extended Data Fig. 3). However, the *adeR* mutant only showed increased sensitivity to benzalkonium and chlorhexidine (Extended Data Fig. 3). These observations align with our TraDIS data and suggest that benzalkonium and chlorhexidine can induce the expression of AdeABC through AdeRS, whereas CTAB, triclosan and chloroxylenol do not act as inducers.

The other important RND system that has been characterized in clinical *A. baumannii* MDR strains is AdeIJK, which share some

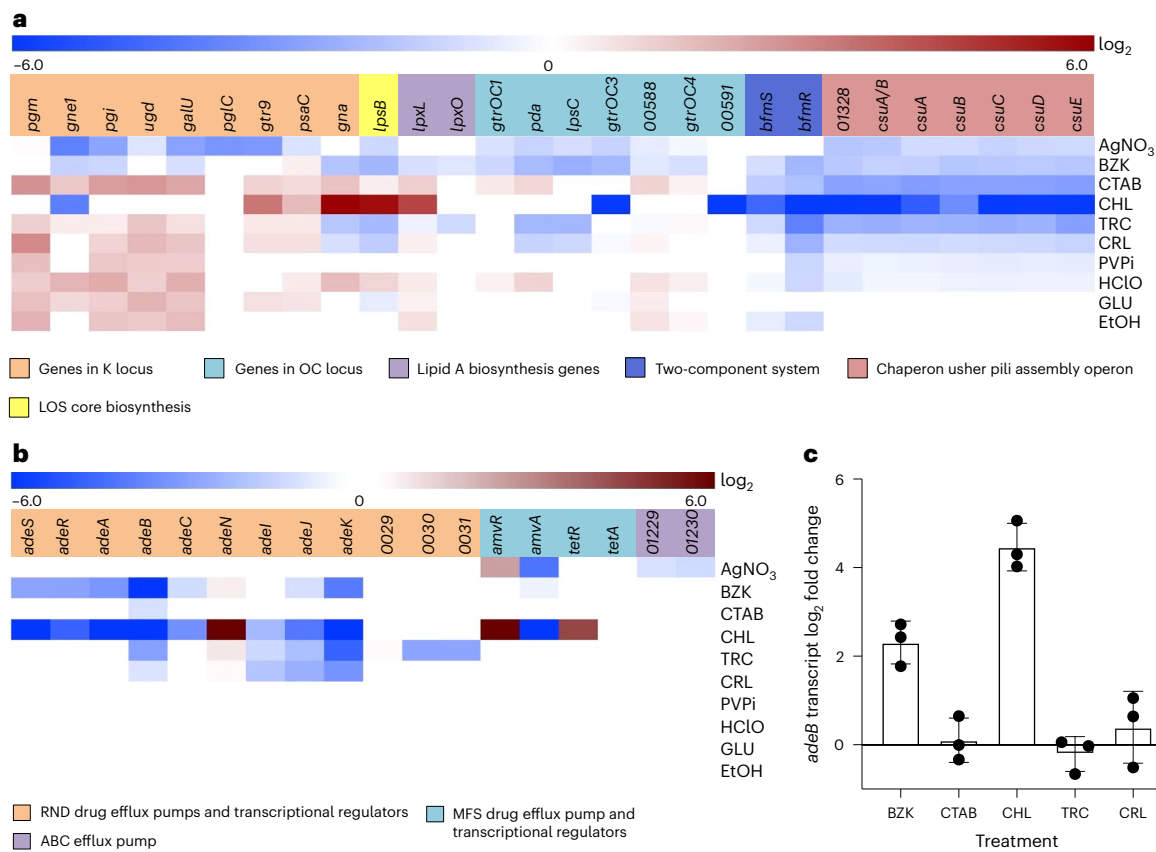


Fig. 2 | Genes with TraDIS insertion changes during biocide exposure. a, Cell envelope-related genes. **b,** Membrane transport-related genes. The colour-coded boxes of the heat map represent the Tn5 insertion read log₂ fold change for each representative gene (above) and for each biocide (right; abbreviations as in Extended Data Table 1), where blue indicates a decrease and red an increase in

Tn5 insertions. Each gene's specific relationship to the cellular function is colour coded, as indicated below the heat map. **c,** Transcriptional response of *adeB* in *A. baumannii* BAL062 to biocides. Data were obtained from three independent biological replicates and are presented as mean ± s.d. The data were processed and plotted using GraphPad Prism v.10.0.0 (131).

substrates with AdeABC^{9,37}. The TraDIS data from this study for *adeJK* are similar to those for *adeABC* (Fig. 2b). For instance, transposon insertions in the OMF gene *adeK* decreased after treatment with AgNO₃, benzalkonium, chlorhexidine, triclosan and chloroxylenol (Fig. 2b). These phenotypes were confirmed by the transposon mutant growth curves of *adeJ* and *adeB* in *A. baumannii* AB5075 (Extended Data Fig. 3). The respective transposon insertion changes in the RND pump gene *adeJ* and MFP gene *adeB* were lower than for *adeK*, suggesting that AdeK might not only form a tripartite drug efflux system with AdeJ and AdeB, but also with AdeAB, consistent with previous reports^{37,38}. *adeN* encodes the transcriptional repressor of *adeJK*³⁹ and showed increased transposon insertion reads after benzalkonium, chlorhexidine, triclosan and chloroxylenol treatment (Fig. 2b).

Tn5 insertions in another RND membrane transporter gene *BAL062_00031* and in the MFP encoding gene *BAL062_00030* were reduced when exposed to triclosan (Fig. 2b). Growth curves showed that the homologue of *BAL062_00031* in *A. baumannii* AB5075 conferred triclosan resistance (Extended Data Fig. 3). There is no OMF gene located adjacent to *BAL062_00030* and *BAL062_00031*. This system may partner with AdeK, because *adeK* is the only OMF gene with reduced insertions (27-fold) after triclosan treatment (Fig. 2b).

Four other drug efflux pumps were also implicated in mediating biocide resistance. The multidrug MFS transporter AmvA can transport benzalkonium and chlorhexidine^{40,41}. Transposon insertions in *amvA* were decreased upon exposure to benzalkonium, chlorhexidine and AgNO₃ (Fig. 2b). The frequency of insertions in *amvR*, encoding

a transcriptional repressor of *amvA*²⁰, increased following exposure to AgNO₃ and chlorhexidine (Fig. 2b). Through growth curves, we confirmed that the *amvA* transposon mutant has lower AgNO₃ resistance than the parental strain (Extended Data Fig. 3), suggesting that AmvA may recognize silver ions as a substrate or may transport other compounds related to silver detoxification.

TetR is a transcriptional repressor of the tetracycline efflux pump gene *tetA*⁴². The transposon insertion reads in *tetR* decreased following exposure to chlorhexidine (Fig. 2b), suggesting that *tetA* overexpression reduces susceptibility to chlorhexidine. In contrast, chlorhexidine did not affect the transposon insertions in *tetA*, which is probably because TetR does not recognize chlorhexidine as a ligand, and it does not induce *tetA* expression. These are consistent with our previous finding that *E. coli* expressing *A. baumannii* TetA increased resistance to chlorhexidine⁴³.

Cell division

Various genes involved in peptidoglycan synthesis, cell shape determination and cell division were shown to have a decreased frequency of Tn5 insertions following treatment with silver nitrate and several other biocides (Extended Data Fig. 4). Insertions in the bacterial rod shape determining genes *mreB*, *mreC*, *mreD*, *rodA* and *pbp2* decreased in frequency upon treatment with AgNO₃. In line with the phenotype of these mutants, Ag⁺ has been shown to cause distortion in bacterial cell membranes and morphology⁴⁴. Hypochlorite and ethanol also caused decreases in the frequency of these mutants (Extended Data Fig. 4), suggesting that they may have similar cellular impacts.

The FtsZ-ring genes (*zipA*, *zapA* and *rlpA*) and 6 genes involved in peptidoglycan synthesis and hydrolysis may have a role in tolerance to multiple biocides (Extended Data Fig. 4). Insertions in *zipA* decreased in frequency when treated with 8 different biocides. The insertion read count of the *pal-tolQ* operon genes, which is required for OM invagination during cell division, was reduced upon chlorhexidine treatment.

Central metabolism and respiration

Several TCA (tricarboxylic acid cycle) cycle genes were impacted by silver nitrate. The frequency of insertions in the TCA cycle genes *sucC* and *sucD* encoding succinyl-CoA synthetase β and α subunits both increased upon AgNO_3 treatment, suggesting that absence of succinyl-CoA synthetase increased resistance to AgNO_3 (Extended Data Fig. 4). Similarly, previous work demonstrated that knockout strains of *E. coli* TCA cycle genes (ΔsucB , Δmdh) were more resistant to AgNO_3 than the parental strain¹¹. In contrast, insertions in two other TCA cycle genes, *acnA_1* (aconitate hydratase) and *icd_2* (isocitrate dehydrogenase), were decreased after AgNO_3 treatment (Extended Data Fig. 4). AgNO_3 may target SuccC/SucD in *A. baumannii*, requiring alteration of fluxes through the TCA cycle such that there is a heavier requirement for *icd_2* and *acnA_1*.

Another known antibacterial effect of AgNO_3 occurs via cytoplasmic membrane proton leakage and attenuated or ceased cell respiration¹². We measured the membrane potential change upon exposure to AgNO_3 in *A. baumannii* BAL062 using 3,3'-diethyloxacarbocyanine iodide ($\text{DiOC}_2(3)$). AgNO_3 at a concentration as low as 1/32 MIC started to cause a dose-dependent drop in the membrane potential of cells in exponential phase (Fig. 3a). The dissipation of membrane potential was reflected in decreased insertions in genes encoding proteins involved in electron/proton shuttling during respiration. For example, Tn5 insertions in *cydB* and *cydA_1* encoding cytochrome D ubiquinol oxidase and in *BAL062_03562* encoding a ubiquinone biosynthesis protein decreased following AgNO_3 treatment (Extended Data Fig. 4). We hypothesize that these genes might be involved in maintaining the PMF (proton motive force) to resist AgNO_3 -induced PMF dissipation.

An operon encoding cytochrome O (*cyo*) ubiquinol oxidase subunits had significantly reduced Tn5 insertions upon chloroxylenol, benzalkonium or ethanol treatment (Extended Data Fig. 4), suggesting that the electron transport chain is affected by these compounds.

Biocide induced dissipation of membrane potential

The finding that cell division and cell respiration genes are required for fitness in the presence of multiple biocides indicated that, similar to AgNO_3 , these molecules may cause dissipation of membrane potential as part of their activity. To explore this hypothesis, we first measured the membrane potential change of *A. baumannii* BAL062 on exposure to AgNO_3 using $\text{DiOC}_2(3)$. As expected, given its known effect causing proton leakage, AgNO_3 caused a drop in cell membrane potential (Fig. 3a). This effect was apparent at a concentration as low as 1/32 MIC and was dose dependent. We then measured the membrane potential of *A. baumannii* BAL062 following exposure to the remaining biocides. On the basis of the importance of cell division and cell respiration genes for fitness in the presence of all biocides except triclosan (Extended Data Fig. 4), we predicted that 9 of the biocides would impact membrane potential. As shown in Fig. 3b, all compounds except for triclosan and ethanol caused a drop in membrane potential. This suggests that dissipation of membrane potential might be a direct or downstream antibacterial effect of multiple biocides.

Cell membrane transport activities are energy dependent. If the biocides in this study do induce dissipation of membrane potential, they should also compromise the solute efflux efficacy of proton-coupled pumps that rely on membrane potential as an energy source. Acriflavine is a passively lipid-membrane-permeable fluorescent compound and a well-known substrate of multiple drug efflux transporters, including AmvA (Extended Data Fig. 5), AdeB and AdeJ⁹ in *A. baumannii*. Its

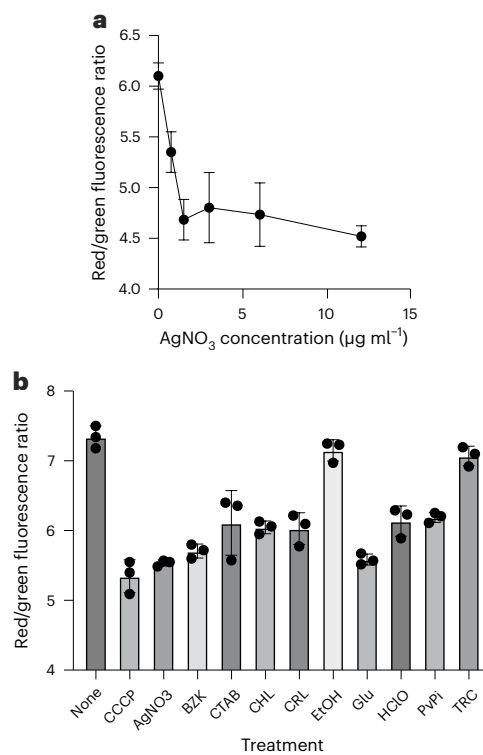


Fig. 3 | Effect of biocides on membrane potential. **a**, Dose-dependent relationship between AgNO_3 and membrane potential in *A. baumannii* BAL062. Values on the X axis are AgNO_3 concentrations (from 1/64 MIC to MIC). Values on the Y axis are the ratios of red versus green fluorescence of $\text{DiOC}_2(3)$, which positively correlate with the cytoplasmic membrane potential. **b**, Biocides induce reduction of membrane potential in *A. baumannii* BAL062. Cells at $\text{OD}_{600} = 0.4–0.6$ were treated with the 10 biocides at 1/4 MIC. CCCP served as a positive control. Data for both panels were obtained from three independent biological replicates and are presented as mean \pm s.d. The data were processed and plotted using GraphPad Prism v.10.0.0 (131).

intracellular accumulation probably correlates with membrane protein efflux activity. We showed that at 1/4 MIC, triclosan and ethanol, the two compounds that did not affect membrane potential, did not change acriflavine fluorescence in *A. baumannii* BAL062. The other 8 compounds and the positive control proton ionophore CCCP (carbonyl cyanide *m*-chlorophenyl hydrazone) increased cellular acriflavine accumulation (Fig. 4b). This suggests that efflux activities in the cells may be compromised due to membrane depolarization caused by these compounds or that transporter substrate competition may lead to less acriflavine efflux. Benzalkonium, chlorhexidine, CTAB, chloroxylenol and triclosan are known substrates of AdeB and AdeJ (Fig. 2b and Extended Data Fig. 2), suggesting that these substrates could compete with acriflavine during the efflux activity of these two transporters. However, triclosan did not affect acriflavine fluorescence, indicating that the elevated acriflavine cellular level was more likely caused by membrane depolarization and a decrease in efflux pump activity. Chlorhexidine and benzalkonium at 1/4 MIC can increase *adeB* expression (Fig. 2c), but rather than triggering the cells to export more acriflavine via AdeB and reducing fluorescence, these biocides increased acriflavine intracellular accumulation (Fig. 4b). These data (Fig. 4b and Fig. 3b) suggest that the 8 biocides, as well as the positive control CCCP, can de-energize the cell membrane and compromise membrane transport.

It is possible that the 8 biocides could be permeabilizing the cell membrane rather than specifically impacting the membrane potential. To investigate this possibility, we examined intracellular fluorescence of SYTOX Green, a fluorescent DNA dye impermeable to intact cell

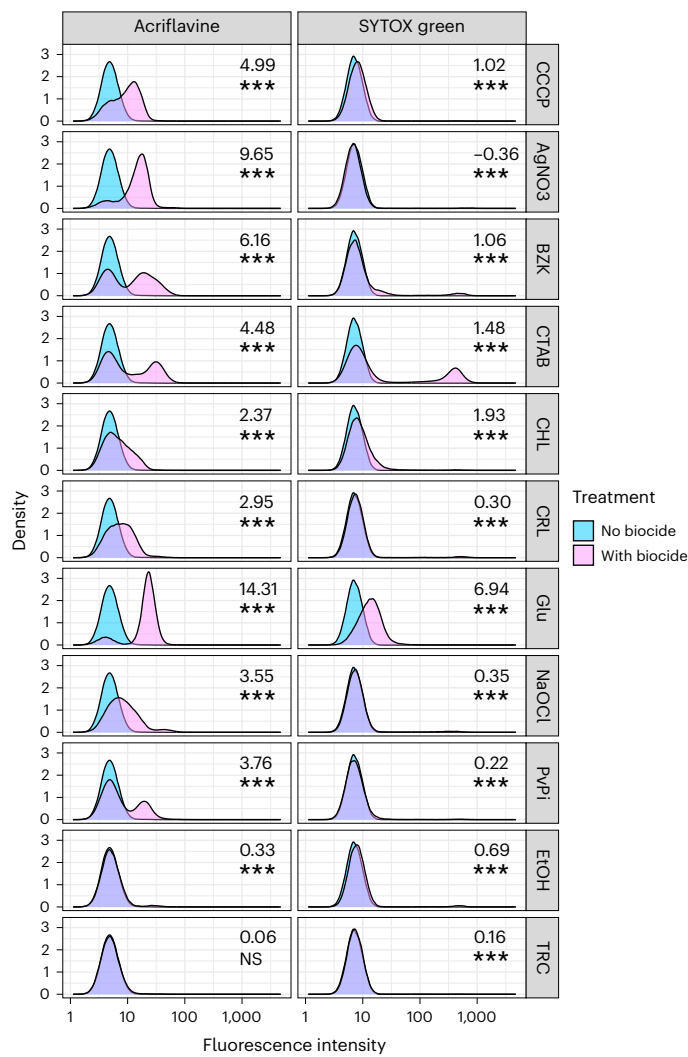


Fig. 4 | Biocides' impact on acriflavine intracellular accumulation and cell membrane permeability. The differences in acriflavine and SYTOX Green accumulation between no treatment and biocide-treated *A. baumannii* BAL062 were measured using flow cytometry (BD Influx cell sorter). The treatment concentration of the 10 biocides was at 1/4 MIC. Each curve shows the fluorescence intensity for around 50,000 cells. Density on the y-axis correlates with cell counts. The cell populations show fluorescence profiles based on the concentration of acriflavine or SYTOX Green in the cell cytoplasm. The mean value of fluorescence intensity difference between no treatment and biocide-treated cells and the statistical significance were measured using one-way analysis of variance (ANOVA) with Dunnett's test; ** $P < 0.001$; *** $P = 0$; NS, not significant. The absolute P values are listed in 2.

membrane. Apart from glutaraldehyde, the other 9 biocides and the positive control CCCP had little effect on SYTOX-Green fluorescence in the cells, suggesting that these compounds at the concentrations tested in this assay do not have an observable impact on cell membrane integrity (Fig. 4b). The observations from both acriflavine and SYTOX Green assays collectively suggest that AgNO_3 , benzalkonium, CTAB, chlorhexidine, chloroxylenol, sodium hypochlorite and povidone iodine (at 1/4 MIC) dissipate the membrane potential without causing systemic membrane damage. In contrast, glutaraldehyde (at 1/4 MIC) permeabilizes the cell membrane, leading to membrane potential dissipation.

Biocide impact on antibiotic potency

The uptake of aminoglycoside antibiotics requires the membrane potential and drug-sensitive ribosomal binding sites for irreversible

drug uptake⁴⁵. Our next hypothesis is that the biocides that cause membrane potential dissipation could compromise aminoglycoside uptake and thus antagonize the killing effects of the antibiotic. As resistant bacterial strains accumulate less aminoglycoside antibiotic than sensitive strains⁴⁶, we used an aminoglycoside-sensitive strain *A. baumannii* ATCC17978 rather than the highly resistant AB5075 or BAL062 strain to test our hypotheses. We showed that apart from triclosan, the other biocides including benzalkonium, chlorhexidine, CTAB and povidone iodine at 1/4 MIC and CCCP increased *A. baumannii* ATCC17978 survival when treated with gentamicin (Fig. 5a). AdeB does not confer resistance to gentamicin³⁷, hence the antagonism with these biocides is unlikely due to drug efflux. Furthermore, *adeB* expression is inducible by benzalkonium and chlorhexidine, but not by CTAB and povidone iodine. Ethanol at 1/4 MIC did not dissipate membrane potential (Fig. 3b), while it did induce gentamicin antagonism (Fig. 5a). The mechanism for ethanol-induced gentamicin antagonism remains unclear. These observations raised the question of whether the biocides can also compromise the antibacterial effects of other antibiotics that have different intracellular targets, such as fluoroquinolones and tetracyclines, or antibiotics that target cell envelopes, such as polymyxins and β -lactams.

Uptake of tetracyclines into the cytoplasm is PMF dependent but probably involves passive diffusion of the uncharged form⁴⁷. Similarly, the zwitterionic form of the fluoroquinolones has been proposed to passively cross the cytoplasmic membrane, but due to their different protonation behaviour from tetracyclines, uptake of some fluoroquinolones has been shown to be negatively correlated with PMF^{47,48}. Benzalkonium and chlorhexidine significantly increased *A. baumannii* survival rates when treated with amikacin (another aminoglycoside), ciprofloxacin (fluoroquinolone) and tigecycline (glycylcycline) (Fig. 5b). In contrast, triclosan had no effect on the efficacy of these antibiotics.

The observed biocide antagonism with amikacin and tigecycline is consistent with our hypothesis that low concentrations of biocides that dissipate the membrane potential will affect uptake and efficacy of antibiotics that have intracellular targets and whose uptake is dependent on the PMF. Although there are differing reports in the literature on whether uptake of fluoroquinolones is dependent on the PMF⁴⁸, our data suggest that ciprofloxacin uptake is PMF dependent.

Dissipation of the membrane potential may not antagonize the antibacterial effects of imipenem and colistin because these antibiotics target the cell envelope. As expected, triclosan, benzalkonium and chlorhexidine have no impact on imipenem killing (Fig. 5b). Synergism was observed between benzalkonium and colistin, but not between triclosan and colistin (Fig. 5b). Chlorhexidine also seemed to marginally enhance colistin killing. The synergy between these compounds is probably because benzalkonium, chlorhexidine and colistin all target cell membranes. Collectively, our data suggest that the biocides that can dissipate membrane potential can promote *A. baumannii* tolerance to various classes of antibiotics that have intracellular targets.

Discussion

TraDIS enabled us to investigate the potential tolerance/resistance determinants and modes of action of 10 diverse biocides that are commonly used as disinfectants. Many of these biocides are known surfactants, causing cell membrane permeabilization and cell lysis, mostly based on biochemistry or phenotypic studies⁵. This study provides additional genetic evidence that these biocides have diverse impacts on the cell surface, including components such as the outer membrane lipooligosaccharide, capsule polysaccharide and chaperone-usher pilus.

We showed that insertions in genes from multiple cellular pathways had statistically significant changes in frequency due to the biocide treatments, including the TCA cycle, electron transport chain and amino acid biosynthesis (Extended Data Fig. 4 and Source Data 1). Non-specific cell membrane disruption has long been proposed to be

the mode of action of charged surfactant biocides, such as chlorhexidine and benzalkonium^{5,49}. Various bacterial drug efflux pumps, including AdeABC, AdeIJK, TetB, AmvA and ABUW_0035 in this study were shown to be tolerance/resistance determinants for multiple biocides.

While antibiotic stewardship has been a topic of increasing public health concern, the debate on whether biocide stewardship is necessary is continuing. Despite some studies reporting increased biocide resistance level in bacterial pathogens in laboratory studies, biocides' in-use concentrations are normally much higher than their minimum bactericidal concentrations and are effective in real-world disinfection practices. There is an increasing number of papers reporting that some biocides, such as benzalkonium, triclosan or heavy metals at sublethal concentrations can promote the emergence of AMR (antimicrobial resistance) pathogens^{50,51}. A recent study further demonstrated that benzalkonium at high dosage can induce persister formation in *E. coli*, which further promotes cell adaptation to various antibiotics⁵².

This study has systematically looked at the effects of biocides at low concentrations. Most of the literature on biocide mechanisms of action dates back to the 1970s and 1980s and has examined the effects of biocides above minimum bactericidal concentration⁵. Our data suggest that residual levels of seven out of ten biocides at sub-MIC levels can dissipate the cellular membrane potential without compromising membrane permeability. The biocide-induced collapse of membrane potential can affect the potency of antibiotics with intracellular targets on bacterial cells, probably by impacting antibiotic uptake. We further showed that the biocides that cause dissipation of the membrane potential promote *A. baumannii* survival rate under treatment with various antibiotics that have intracellular targets, including aminoglycosides, ciprofloxacin and tigecycline. However, the biocides do not antagonize the killing effects of drugs targeting the cell envelope, such as colistin and imipenem.

Although drug efflux pumps generally confer low-level resistance to antibiotics, compared with their parental strains, bacteria that lack key MDR efflux systems are much less likely to develop MDR^{53,54}. Furthermore, intermittent antibiotic exposures have been shown to lead to more rapid evolution of tolerance and resistance^{55–57} and antibiotic tolerance facilitates the AMR evolution⁵⁸. These studies and our data together suggest that factors affecting antibiotic intracellular accumulation are important in AMR development. Previous studies have typically used direct measurement of bacterial susceptibilities to antibiotics and biocides to investigate co-selection of antibiotic resistance. We propose that the principal concern with respect to biocide stewardship is not the emergence of biocide resistance or antibiotic cross-resistance, but rather the presence of residual biocides, especially chlorhexidine, benzalkonium, CTAB and others that are hard to remove from the environment, could induce antibiotic tolerance and AMR development.

Methods

Bacterial strains and mutant library

The *A. baumannii* global clonal II MDR strain BAL062 (ENA accession numbers [LT594095](#) to [LT594096](#)) was used as the parental strain for mutant library construction, yielding a saturated Tn5 mutant library containing >100,000 unique mutants. The Tn5 transposome was custom built by using the EZ-Tn5 custom transposome construction kit (Epicentre) and a kanamycin-resistant gene cassette that was amplified from pUT-km1 plasmid. The custom transposome was electroporated into BAL062 in a 0.1 mm cuvette (Gene Pulser Xcell Total System, Bio-Rad) and the cells were selected on kanamycin (10 mg l⁻¹) agar plates and incubated at 37 °C overnight. The mutants (>100,000 c.f.u.) were collected and stored as glycerol stocks at -80 °C. On average, among the non-essential genes (*n* = 3,362) in this Tn5 mutant library, there were 35.9 unique insertions per kb of gene sequence. *A. baumannii* AB5075-UW wild type and Tn26 insertion mutants were obtained from the Manoil lab collection⁵⁹ (Extended Data Table 3).

Biocides and biocide-susceptibility test

The MICs of the parental strain *A. baumannii* BAL062 against 10 biocides (Extended Data Table 2) were tested through the 2-fold serial broth dilution method in cation-adjusted Mueller-Hinton II (MHII) medium (BD Biosciences). The 10 biocides were silver nitrate (Sigma-Aldrich, S6506), benzalkonium chloride (Sigma-Aldrich, 12060), chlorhexidine diacetate (Sigma-Aldrich, C1520000), Cetyl-trimethylammonium bromide (Sigma-Aldrich, 219374), triclosan (Sigma-Aldrich, 72779), chloroxylenol (Sigma-Aldrich, PHR1478), polyvidone iodine (Sigma-Aldrich, Y0000466), sodium hypochlorite (Sigma-Aldrich, 13440), 50 wt % glutaraldehyde in water (Sigma-Aldrich, 340855) and 100% ethanol (Chem-supply, EL043). Due to the different solubilities of the compounds, the media used were varied. Triclosan and chloroxylenol were tested in MHII supplemented with DMSO, AgNO₃ in Luria Bertani (LB) broth without sodium chloride and the remaining compounds in MHII broth. Three biological repeats were performed to confirm MIC values.

Growth curve assay

For the phenotypes undetectable by the MIC, growth curve assays were performed to validate biocide fitness levels of the transposon mutants. Overnight cultures of *A. baumannii* AB5075 parental strain and the derivative transposon mutants were subcultured at 1:100 in MHII broth and grown at 37 °C with shaking at 200 r.p.m. When the cell density reached OD₆₀₀ = 0.5–0.6, the cell culture was diluted in fresh MHII broth supplemented with biocides of interest in a 96-well plate, with final cell density pf $\sim 10^5$ c.f.u. ml⁻¹. The plate was incubated in a BMG LABTECH PHERAstar FS plate reader and optical density data over 24 h were collected. Growth curve data of three biological replicates of each treatment condition were processed and plotted using GraphPad Prism 10.0.0 (131).

TraDIS assay

For each biocide, two biological replicates of $\sim 1 \times 10^9$ cells of *A. baumannii* BAL062 mutant TraDIS library were inoculated into each 10 ml of growth medium and grown for 16 h at 37 °C with shaking at 200 r.p.m., yielding 18 sets that were in MHII broth, 6 sets in DMSO-complemented MHII broth and 4 sets in LB broth without sodium chloride. The overnight cultures were diluted 1/100 in the same fresh media, which were then inoculated with respective biocide compounds at 1/4 MIC (Extended Data Table 2), or without treatment for the 6 negative controls, and grown at 37 °C with shaking at 200 r.p.m. for 16 h. The genomic DNA (gDNA) from 2 ml of the overnight cultures was extracted and purified using DNeasy blood and tissue kit (Qiagen, 69506).

TraDIS sequencing and data analysis

Genomic DNA (5 µg) was fragmented for each of the 28 TraDIS assay gDNA samples, and TraDIS sequencing libraries were constructed according to standardized protocol²¹. TraDIS sequencing was performed on a HiSeq2500 Illumina platform and generated 500,000k 50 bp single-end reads per sample. The resulting FASTQ files and transposon insertion read mapping were analysed as described in the TraDIS Toolkit²¹. The primers used for transposon insertion-site enrichment and TraDIS sequencing are listed in Supplementary Table 1.

Membrane potential assay via flow cytometry

Membrane potential was assessed using the BacLight bacterial membrane potential kit (ThermoFisher, [B34950](#)). Multiple colonies of *A. baumannii* BAL062 were inoculated into 5 ml growth media in 50-ml Falcon tubes, including three biological replicates, which were incubated at 37 °C with shaking at 200 r.p.m. overnight or for 16 h. Of the overnight cultures, 50 µl were inoculated into 5 ml fresh media in 50-ml Falcon tubes or cell culture flasks and incubated at 37 °C with shaking at 200 r.p.m. until the cells reached early (OD₆₀₀ = 0.4–0.6) exponential phase. AgNO₃ media was in LB without sodium chloride,

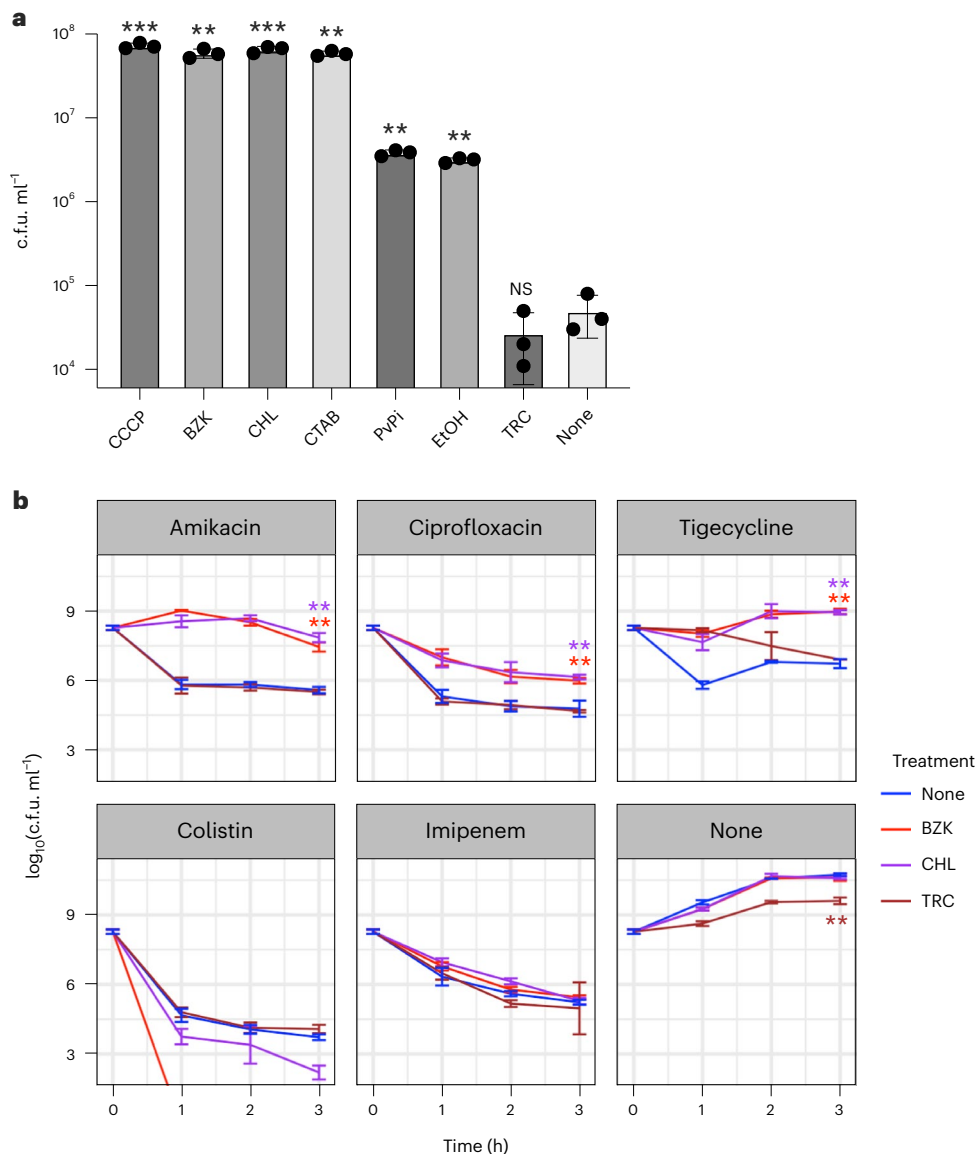


Fig. 5 | Biocides and antibiotics interactions in *A. baumannii*. a, Biocides that dissipate membrane potential also reduce gentamicin potency. Statistical significance was assessed using one-way ANOVA. **b**, Biocide antagonism with a broader range of antibiotics of intracellular targets. Statistical significance overall was assessed using mixed repeated-measures ANOVA, followed by a

one-way ANOVA with Dunnett's post hoc test at $t = 3$ if the first test showed a significant effect. All data in both panels are presented as mean \pm s.d.; ** $P < 0.01$ and *** $P < 0.001$, from three independent biological replicates. The absolute P values are listed in 4.

and the media for all the other biocide membrane potential assays were prepared in MHII broth. Cell cultures that reached the designated density were treated with biocide at 1/4 MIC (Extended Data Table 2) for 2–5 min at 37 °C with shaking at 200 r.p.m. Then, 10 μ l of the culture was inoculated in 1 ml sterile-filtered phosphate buffered saline (PBS) (Sigma-Aldrich, P4417) that was supplemented with 8 μ g ml^{-1} DiOC₂(3), incubated at room temperature for up to 30 min and then analysed by flow cytometry in a BD Influx cell sorter. When excited by blue laser (488 nm), DiOC₂(3) has peak emission wavelengths at 530 nm (FITC) and 610 nm (Texas Red). The samples treated with DiOC₂(3) were compared to the samples without treatment to confirm that the fluorescent signals detected in FITC and Texas Red channels were from DiOC₂(3) and to gate the cell population of interest. Of the gated population, 50,000 events were collected for each sample. The red/green fluorescence intensity ratio that is proportional to membrane potential was calculated on the basis of the total events for each sample. The gating strategy and control justification are presented in Extended Data Fig. 6.

Acriflavine cellular accumulation assay and membrane permeability assay via flow cytometry

Overnight cultures of *A. baumannii* BAL062 were prepared as described in 'Membrane potential assay via flow cytometry', subcultured at 1:100 in respective growth media and grown at 37 °C with shaking at 200 r.p.m. until OD₆₀₀ reached 0.4–0.6. For the acriflavine (Sigma-Aldrich, A8126) cellular accumulation assay, biocides at 1/4 MIC and acriflavine at 1/32 MIC (Extended Data Table 2) were then added to the cultures that were then incubated at 37 °C with shaking at 200 r.p.m. for 2–5 min. The cultures were then diluted 1/100 in fresh growth media supplemented with acriflavine at 1/32 MIC immediately before flow cytometry analysis in the BD Influx cell sorter, at an excitation wavelength of 488 nm and emission wavelength of 530 nm. For the membrane permeability assay, biocides at 1/4 MIC and 1 μ M SYTOX Green (ThermoFisher, S7020) were added to the subculture, which was then incubated at 37 °C with shaking at 200 r.p.m. for 2–5 min. The cultures were diluted 1/100 in fresh growth media supplemented

with 1 µM SYTOX Green immediately before flow cytometry analysis in the BD Influx cell sorter, at an excitation wavelength of 488 nm and emission wavelength of 530 nm. Non-stained samples were also analysed in the BD Influx cell sorter to assist in gating the cell population of interest. Of the gated population, 50,000 events were collected for each sample in both assays. The gating strategy and control justification are presented in the Extended Data Fig. 7.

RT-qPCR

Wild-type *A. baumannii* BAL062 was grown to OD₆₀₀ = 0.5–0.6 and treated with the biocides benzalkonium, chlorhexidine, CTAB, chloroxylenol and triclosan at 1/4 MIC for 30 min. Three independent biological replicates were included. Total RNA was extracted using the QIAGEN RNeasy mini kit (74104). The residual gDNA was removed using TURBO DNase (2 U µl⁻¹) (ThermoFisher, AM2238). The messenger RNA of *adeB* and the housekeeping gene *gapdh* were reverse transcribed and the relative transcriptional-level differences of these two genes among the biocide treatments were determined using KAPA SYBR FAST One-Step RT-qPCR Master Mix (2X) kit (MERCK, KK4650) in a ROCHE LightCycler 480 system. The primers used here are listed in Supplementary Table 1.

Antimicrobial killing assay

To examine the effect of biocides on gentamicin killing, overnight cultures of *A. baumannii* ATCC17978 (incubated in 50-ml Falcon tubes) were subcultured at 1:100 in fresh MHII medium and grown at 37 °C with shaking at 200 r.p.m. to an OD₆₀₀ of 0.6–0.8. Biocides at 1/4 MIC and gentamicin at 2× MIC were sequentially added to the cultures at room temperature. The cultures were returned to incubation at 37 °C with shaking at 200 r.p.m., and were then serially diluted and plated to enumerate viable bacteria after 60 min. The effect of biocides on killing by amikacin, ciprofloxacin, tigecycline, colistin and imipenem was measured similarly, except that cells were grown to an OD₆₀₀ of 0.4–0.6 and survival was measured at 1, 2 and 3 h post treatment. The concentrations of biocides and antibiotics are listed in the Extended Data Table 2.

Statistics and reproducibility

The significance of gene read count differences of TraDIS data was processed and predicted using *tradis_comparisons.R*, which provides insight on genes that contribute to *A. baumannii* fitness to the biocides tested²¹. The remaining experiments included three random independent biological replicates. No statistical method was used to predetermine sample size and no data were excluded from the analyses.

Reporting summary

Further information on research design is available in the Nature Portfolio Reporting Summary linked to this article.

Data availability

TraDIS sequencing data were deposited in the European Nucleotide Database under project number PRJEB8707. Source data are provided with this paper.

References

- O’Neil, J. *Tackling a Crisis for the Health and Wealth of Nations* (World Health Organization, 2014).
- Darby, E. M. et al. Molecular mechanisms of antibiotic resistance revisited. *Nat. Rev. Microbiol.* **21**, 280–295 (2023).
- Peleg, A. Y., Seifert, H. & Paterson, D. L. *Acinetobacter baumannii*: emergence of a successful pathogen. *Clin. Microbiol. Rev.* **21**, 538–582 (2008).
- Wong, D. et al. Clinical and pathophysiological overview of *Acinetobacter* infections: a century of challenges. *Clin. Microbiol. Rev.* **30**, 409–447 (2017).
- McDonnell, G. & Russell, A. D. Antiseptics and disinfectants: activity, action, and resistance. *Clin. Microbiol. Rev.* **12**, 147–179 (1999).
- Webber, M. A. et al. Parallel evolutionary pathways to antibiotic resistance selected by biocide exposure. *J. Antimicrob. Chemother.* **70**, 2241–2248 (2015).
- Fernández-Cuenca, F. et al. Reduced susceptibility to biocides in *Acinetobacter baumannii*: association with resistance to antimicrobials, epidemiological behaviour, biological cost and effect on the expression of genes encoding porins and efflux. *J. Antimicrob. Chemother.* **70**, 3222–3229 (2015).
- Alekshun, M. N. & Levy, S. B. The mar regulon: multiple resistance to antibiotics and other toxic chemicals. *Trends Microbiol.* **7**, 410–413 (1999).
- Rajamohan, G., Srinivasan, V. B. & Gebreyes, W. A. Novel role of *Acinetobacter baumannii* RND efflux transporters in mediating decreased susceptibility to biocides. *J. Antimicrob. Chemother.* **65**, 228–232 (2010).
- Liau, S. Y., Read, D. C., Pugh, W. J., Furr, J. R. & Russell, A. D. Interaction of silver nitrate with readily identifiable groups: relationship to the antibacterial action of silver ions. *Lett. Appl. Microbiol.* **25**, 279–283 (1997).
- Morones-Ramirez, J. R., Winkler, J. A., Spina, C. S. & Collins, J. J. Silver enhances antibiotic activity against Gram-negative bacteria. *Sci. Transl. Med.* **5**, 190ra181 (2013).
- Dibrov, P., Dzioba, J., Gosink, K. K. & Häse, C. C. Chemiosmotic mechanism of antimicrobial activity of Ag(+) in *Vibrio cholerae*. *Antimicrob. Agents Chemother.* **46**, 2668–2670 (2002).
- Gupta, A., Matsui, K., Lo, J. F. & Silver, S. Molecular basis for resistance to silver cations in *Salmonella*. *Nat. Med.* **5**, 183–188 (1999).
- Franke, S., Grass, G. & Nies, D. H. The product of the ybdE gene of the *Escherichia* chromosome is involved in detoxification of silver ions. *Microbiology* **147**, 965–972 (2001).
- McMurtry, L. M., Oethinger, M. & Levy, S. B. Triclosan targets lipid synthesis. *Nature* **394**, 531–532 (1998).
- Chen, Y., Pi, B., Zhou, H., Yu, Y. & Li, L. Triclosan resistance in clinical isolates of *Acinetobacter baumannii*. *J. Med. Microbiol.* **58**, 1086–1091 (2009).
- Hassan, K. A., Liu, Q., Henderson, P. J. F. & Paulsen, I. T. Homologs of the *Acinetobacter baumannii* Acel transporter represent a new family of bacterial multidrug efflux systems. *mBio* **6**, e01982-14 (2015).
- Langridge, G. C. et al. Simultaneous assay of every *Salmonella* Typhi gene using one million transposon mutants. *Genome Res.* **19**, 2308–2316 (2009).
- Cain, A. K. et al. A decade of advances in transposon-insertion sequencing. *Nat. Rev. Genet.* **21**, 526–540 (2020).
- Hassan, K. A. et al. Fluorescence-based flow sorting in parallel with transposon insertion site sequencing identifies multidrug efflux systems in *Acinetobacter baumannii*. *mBio* **7**, e01200-16 (2016).
- Barquist, L. et al. The TraDIS toolkit: sequencing and analysis for dense transposon mutant libraries. *Bioinformatics* **32**, 1109–1111 (2016).
- Hood, M. I., Becker, K. W., Roux, C. M., Dunman, P. M. & Skaar, E. P. Genetic determinants of intrinsic colistin tolerance in *Acinetobacter baumannii*. *Infect. Immun.* **81**, 542–551 (2013).
- Turnbough, C. L. & Switzer, R. L. Regulation of pyrimidine biosynthetic gene expression in bacteria: repression without repressors. *Microbiol. Mol. Biol. Rev.* **72**, 266–300 (2008).
- Kenyon, J. J., Nigro, S. J. & Hall, R. M. Variation in the OC locus *Acinetobacter baumannii* genomes predicts extensive structural diversity in the lipoooligosaccharide. *PLoS ONE* **9**, e107833 (2014).

25. Arroyo, L. A. et al. The pmrCAB operon mediates polymyxin resistance in *Acinetobacter baumannii* ATCC 17978 and clinical isolates through phosphoethanolamine modification of lipid A. *Antimicrob. Agents Chemother.* **55**, 3743–3751 (2011).
26. Boll, J. M. et al. Reinforcing lipid A acylation on the cell surface of *Acinetobacter baumannii* promotes cationic antimicrobial peptide resistance and desiccation survival. *mBio* **6**, e00478-15 (2015).
27. Kenyon, J. J. & Hall, R. M. Variation in the complex carbohydrate biosynthesis loci of *Acinetobacter baumannii* genomes. *PLoS ONE* **8**, e62160 (2013).
28. Lees-Miller, R. G. et al. A common pathway for O-linked protein-glycosylation and synthesis of capsule in *Acinetobacter baumannii*. *Mol. Microbiol.* **89**, 816–830 (2013).
29. Geisinger, E. & Isberg, R. R. Antibiotic modulation of capsular exopolysaccharide and virulence in *Acinetobacter baumannii*. *PLoS Pathog.* **11**, e1004691 (2015).
30. Luke, N. R. et al. Identification and characterization of a glycosyl-transferase involved in *Acinetobacter baumannii* lipopolysaccharide core biosynthesis. *Infect. Immun.* **78**, 2017–2023 (2010).
31. Kenyon, J. J., Holt, K. E., Pickard, D., Dougan, G. & Hall, R. M. Insertions in the OCL1 locus of *Acinetobacter baumannii* lead to shortened lipooligosaccharides. *Res. Microbiol.* **165**, 472–475 (2014).
32. Pakharukova, N. et al. Structural insight into archaic and alternative chaperone-usher pathways reveals a novel mechanism of pilus biogenesis. *PLoS Pathog.* **11**, e1005269 (2015).
33. Coyne, S., Courvalin, P. & Périchon, B. Efflux-mediated antibiotic resistance in *Acinetobacter* spp. *Antimicrob. Agents Chemother.* **55**, 947–953 (2011).
34. Magnet, S., Courvalin, P. & Lambert, T. Resistance-nodulation-cell division-type efflux pump involved in aminoglycoside resistance in *Acinetobacter baumannii* strain BM4454. *Antimicrob. Agents Chemother.* **45**, 3375–3380 (2001).
35. Yoon, E. J., Courvalin, P. & Grillot-Courvalin, C. RND-type efflux pumps in multidrug-resistant clinical isolates of *Acinetobacter baumannii*: major role for AdeABC overexpression and AdeRS mutations. *Antimicrob. Agents Chemother.* **57**, 2989–2995 (2013).
36. Hassan, K. A. et al. Transcriptomic and biochemical analyses identify a family of chlorhexidine efflux proteins. *Proc. Natl Acad. Sci. USA* **110**, 20254–20259 (2013).
37. Sugawara, E. & Nikaido, H. Properties of AdeABC and AdelJK efflux systems of *Acinetobacter baumannii* compared with those of the AcrAB-TolC system of *Escherichia coli*. *Antimicrob. Agents Chemother.* **58**, 7250–7257 (2014).
38. Leus, I. V. et al. Substrate specificities and efflux efficiencies of RND efflux pumps of *Acinetobacter baumannii*. *J. Bacteriol.* <https://doi.org/10.1128/JB.00049-18> (2018).
39. Rosenfeld, N., Bouchier, C., Courvalin, P. & Périchon, B. Expression of the resistance-nodulation-cell division pump AdelJK in *Acinetobacter baumannii* is regulated by AdeN, a TetR-type regulator. *Antimicrob. Agents Chemother.* **56**, 2504–2510 (2012).
40. Rajamohan, G., Srinivasan, V. B. & Gebreyes, W. A. Molecular and functional characterization of a novel efflux pump, AmvA, mediating antimicrobial and disinfectant resistance in *Acinetobacter baumannii*. *J. Antimicrob. Chemother.* **65**, 1919–1925 (2010).
41. Hassan, K. A. et al. Roles of DHA2 family transporters in drug resistance and iron homeostasis in *Acinetobacter* spp. *J. Mol. Microbiol. Biotechnol.* **20**, 116–124 (2011).
42. Orth, P., Schnappinger, D., Hillen, W., Saenger, W. & Hinrichs, W. Structural basis of gene regulation by the tetracycline inducible Tet repressor-operator system. *Nat. Struct. Biol.* **7**, 215–219 (2000).
43. Li, L., Hassan, K. A., Brown, M. H. & Paulsen, I. T. Rapid multiplexed phenotypic screening identifies drug resistance functions for three novel efflux pumps in *Acinetobacter baumannii*. *J. Antimicrob. Chemother.* **71**, 1223–1232 (2016).
44. Jung, W. K. et al. Antibacterial activity and mechanism of action of the silver ion in *Staphylococcus aureus* and *Escherichia coli*. *Appl. Environ. Microbiol.* **74**, 2171–2178 (2008).
45. Taber, H. W., Mueller, J. P., Miller, P. F. & Arrow, A. S. Bacterial uptake of aminoglycoside antibiotics. *Microbiol. Rev.* **51**, 439–457 (1987).
46. Holtje, J. V. Induction of streptomycin uptake in resistant strains of *Escherichia coli*. *Antimicrob. Agents Chemother.* **15**, 177–181 (1979).
47. Nikaido, H. & Thanassi, D. G. Penetration of lipophilic agents with multiple protonation sites into bacterial cells: tetracyclines and fluoroquinolones as examples. *Antimicrob. Agents Chemother.* **37**, 1393–1399 (1993).
48. Piddock, L. J. Mechanism of quinolone uptake into bacterial cells. *J. Antimicrob. Chemother.* **27**, 399–403 (1991).
49. Morente, E. O. et al. Biocide tolerance in bacteria. *Int. J. Food Microbiol.* **162**, 13–25 (2013).
50. Zhao, Y. et al. Evidence for co-selection of antibiotic resistance genes and mobile genetic elements in metal polluted urban soils. *Sci. Total Environ.* **656**, 512–520 (2019).
51. Short, F. L. et al. Benzalkonium chloride antagonises aminoglycoside antibiotics and promotes evolution of resistance. *Ebiomedicine* <https://doi.org/10365310.1016/j.ebiom.2021.103653> (2021).
52. Nordholt, N., Kanaris, O., Schmidt, S. B. I. & Schreiber, F. Persistence against benzalkonium chloride promotes rapid evolution of tolerance during periodic disinfection. *Nat. Commun.* **12**, 6792 (2021).
53. Papkou, A., Hedge, J., Kapel, N., Young, B. & MacLean, R. C. Efflux pump activity potentiates the evolution of antibiotic resistance across *S. aureus* isolates. *Nat. Commun.* **11**, 3970 (2020).
54. El Meouche, I. & Dunlop, M. J. Heterogeneity in efflux pump expression predisposes antibiotic-resistant cells to mutation. *Science* **362**, 686–690 (2018).
55. Fridman, O., Goldberg, A., Ronin, I., Shores, N. & Balaban, N. Q. Optimization of lag time underlies antibiotic tolerance in evolved bacterial populations. *Nature* **513**, 418–421 (2014).
56. Van den Bergh, B. et al. Frequency of antibiotic application drives rapid evolutionary adaptation of *Escherichia coli* persistence. *Nat. Microbiol.* **1**, 16020 (2016).
57. Baym, M. et al. Spatiotemporal microbial evolution on antibiotic landscapes. *Science* **353**, 1147–1151 (2016).
58. Levin-Reisman, I. et al. Antibiotic tolerance facilitates the evolution of resistance. *Science* **355**, 826–830 (2017).
59. Gallagher, L. A. et al. Resources for genetic and genomic analysis of emerging pathogen *Acinetobacter baumannii*. *J. Bacteriol.* **197**, 2027–2035 (2015).
60. Odermatt, A., Krapf, R. & Solioz, M. Induction of the putative copper ATPase, CopA and CopB, of *Enterococcus hirae* by Ag⁺ and Cu²⁺ extrusion by CopB. *Biochem. Biophys. Res. Commun.* **202**, 44–48 (1994).
61. Maillard, J. Y. & Hartemann, P. Silver as an antimicrobial: facts and gaps in knowledge. *Crit. Rev. Microbiol.* **39**, 473–483 (2013).
62. Srinivasan, V. B., Rajamohan, G. & Gebreyes, W. A. Role of AbeS, a novel efflux pump of the SMR family of transporters, in resistance to antimicrobial agents in *Acinetobacter baumannii*. *Antimicrob. Agents Chemother.* **53**, 5312–5316 (2009).
63. Ogase, H., Nagai, I., Kameda, K., Kume, S. & Ono, S. Identification and quantitative analysis of degradation products of chlorhexidine with chlorhexidine-resistant bacteria with three-dimensional high performance liquid chromatography. *J. Appl. Bacteriol.* **73**, 71–78 (1992).
64. Su, X. Z., Chen, J., Mizushima, T., Kuroda, T. & Tsuchiya, T. AbeM, an H⁺-coupled *Acinetobacter baumannii* multidrug efflux pump belonging to the MATE family of transporters. *Antimicrob. Agents Chemother.* **49**, 4362–4364 (2005).

65. Zhu, L., Lin, J., Ma, J., Cronan, J. E. & Wang, H. Triclosan resistance of *Pseudomonas aeruginosa* PAO1 is due to FabV, a triclosan-resistant enoyl-acyl carrier protein reductase. *Antimicrob. Agents Chemother.* **54**, 689–698 (2010).
66. Chesney, J. A., Eaton, J. W. & Mahoney, J. R. Bacterial glutathione: a sacrificial defense against chlorine compounds. *J. Bacteriol.* **178**, 2131–2135 (1996).
67. Fried, V. A. & Novick, A. Organic solvents as probes for the structure and function of the bacterial membrane: effects of ethanol on the wild type and an ethanol-resistant mutant of *Escherichia coli* K-12. *J. Bacteriol.* **114**, 239–248 (1973).

Acknowledgements

This work was supported by NHMRC (National Health and Medical Research Council) project grants APP1127615, APP1060895 and APP1165135 to I.T.P. and K.A.H. This work was also supported by ARC (Australian Research Council) Centre of Excellence in Synthetic Biology grant CE200100029 to I.T.P. The sequencing was supported by Wellcome Trust grant WT098051. Construction of the transposon mutant library was supported by Wellcome Trust grant WT100087/Z/12/Z. I.T.P. was supported by ARC Laureate Fellowship FL140100021. A.K.C. was supported by ARC DECRA (Discovery Early Career Research Award) Fellowship DE180100929. F.L.S. was supported by ARC DECRA Fellowship DE200101524. K.A.H. was supported by ARC Future Fellowship FT180100123.

Author contributions

I.T.P., K.A.H. and L.L. conceptualized this project. S.B. constructed the *A. baumannii* transposon mutant library. L.L. performed TraDIS assays. A.K.C. and J.P. developed and performed TraDIS sequencing, transposon insertion read mapping and statistical analysis. L.L. and A.K.C. analysed TraDIS data. L.L. formed hypotheses including that biocides dissipate membrane potential. I.T.P., F.L.S. and L.L. formed the hypothesis of the antagonism between biocides and antibiotics. L.L., F.L.S., V.N., A.P., S.S.N., F.T.P., B.S.S. and N.A. performed the follow-up

experiments. L.L., I.T.P. and A.K.C. wrote the manuscript. K.A.H., F.L.S. and J.P. reviewed and improved the manuscript.

Competing interests

The authors declare no competing interests.

Additional information

Extended data is available for this paper at <https://doi.org/10.1038/s41564-023-01474-z>.

Supplementary information The online version contains supplementary material available at <https://doi.org/10.1038/s41564-023-01474-z>.

Correspondence and requests for materials should be addressed to Amy K. Cain or Ian T. Paulsen.

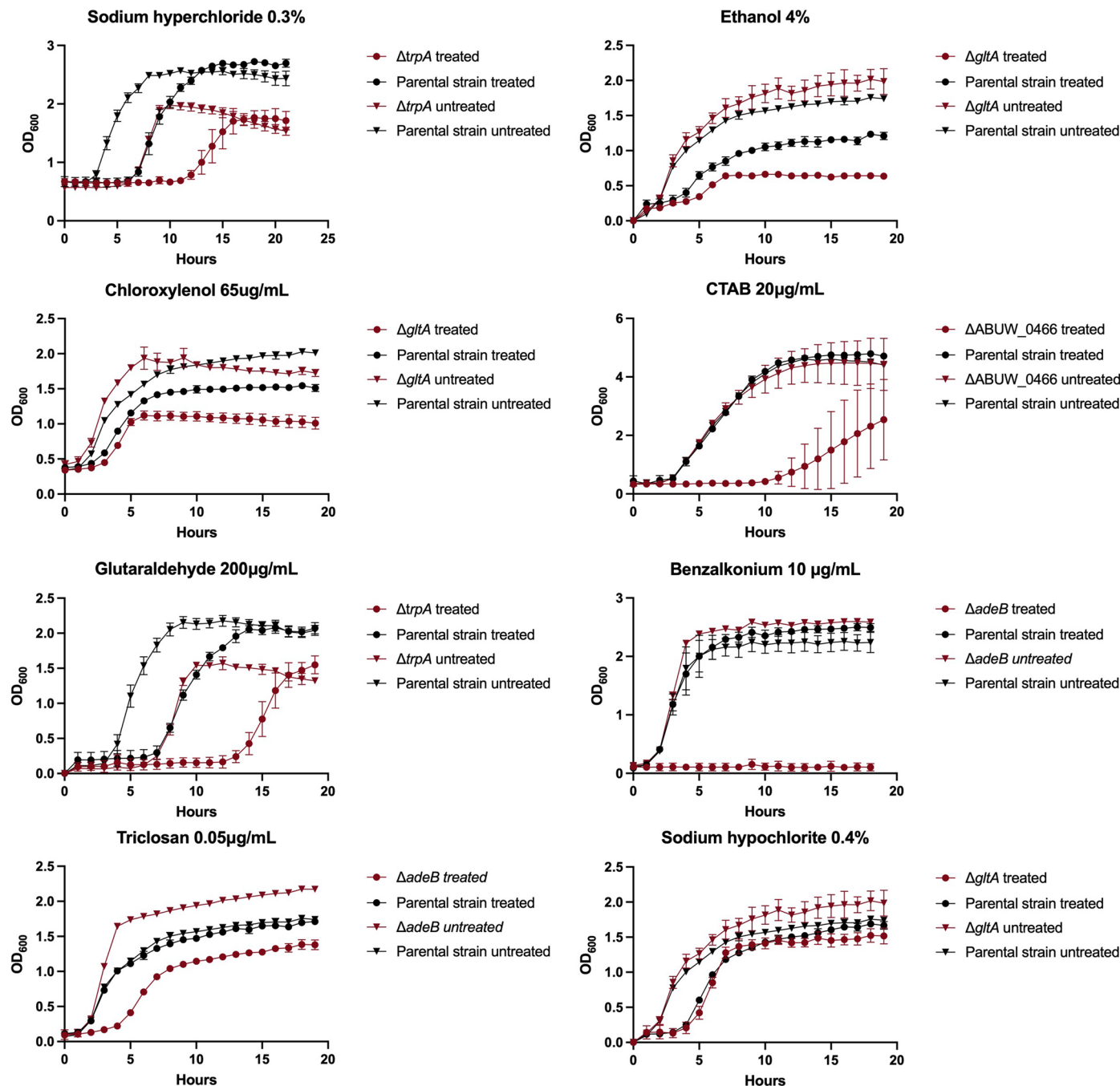
Peer review information *Nature Microbiology* thanks Nicholas Jakubovics, Jessica Blair and the other, anonymous, reviewer(s) for their contribution to the peer review of this work.

Reprints and permissions information is available at www.nature.com/reprints.

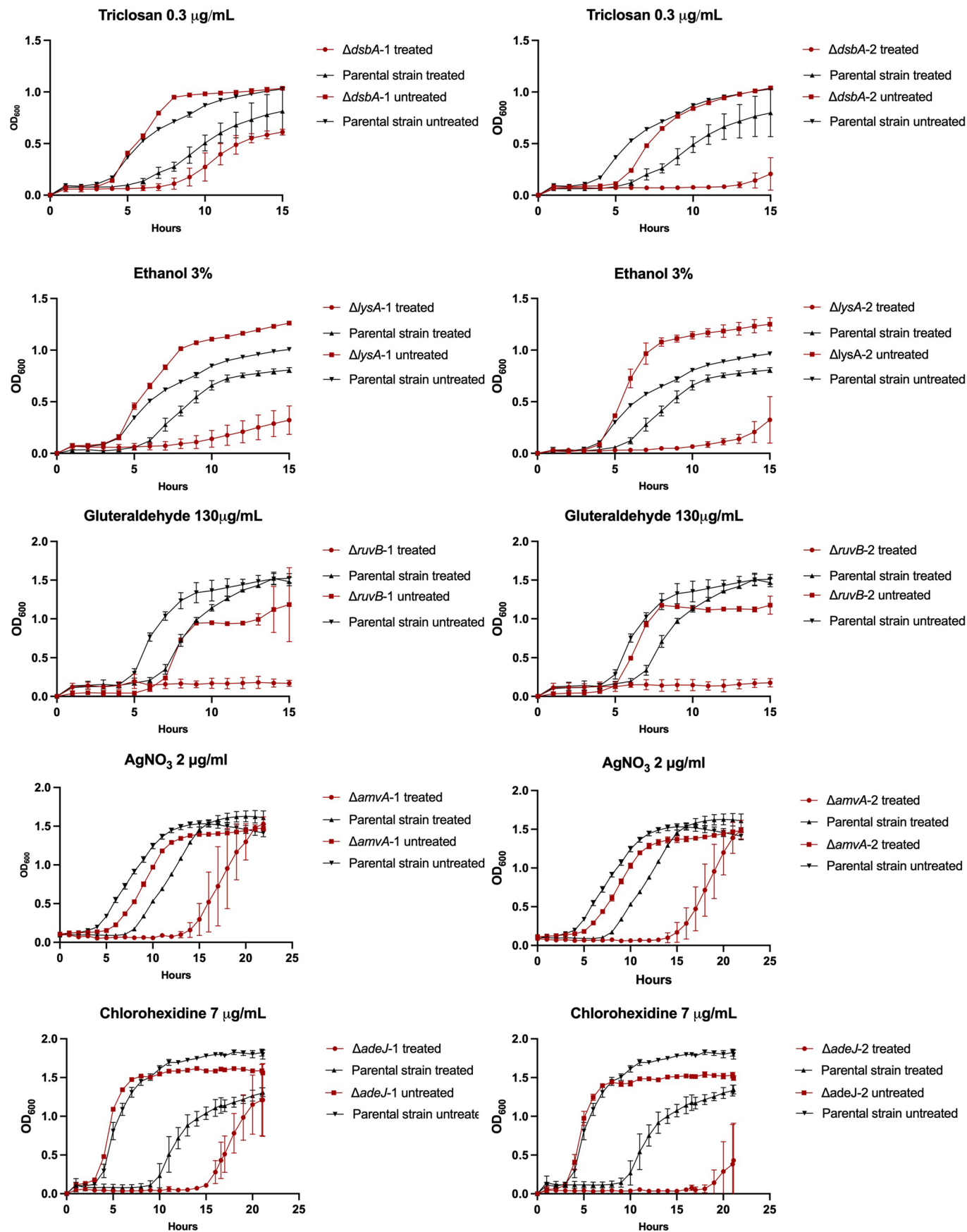
Publisher's note Springer Nature remains neutral with regard to jurisdictional claims in published maps and institutional affiliations.

Springer Nature or its licensor (e.g. a society or other partner) holds exclusive rights to this article under a publishing agreement with the author(s) or other rightsholder(s); author self-archiving of the accepted manuscript version of this article is solely governed by the terms of such publishing agreement and applicable law.

© The Author(s), under exclusive licence to Springer Nature Limited 2023



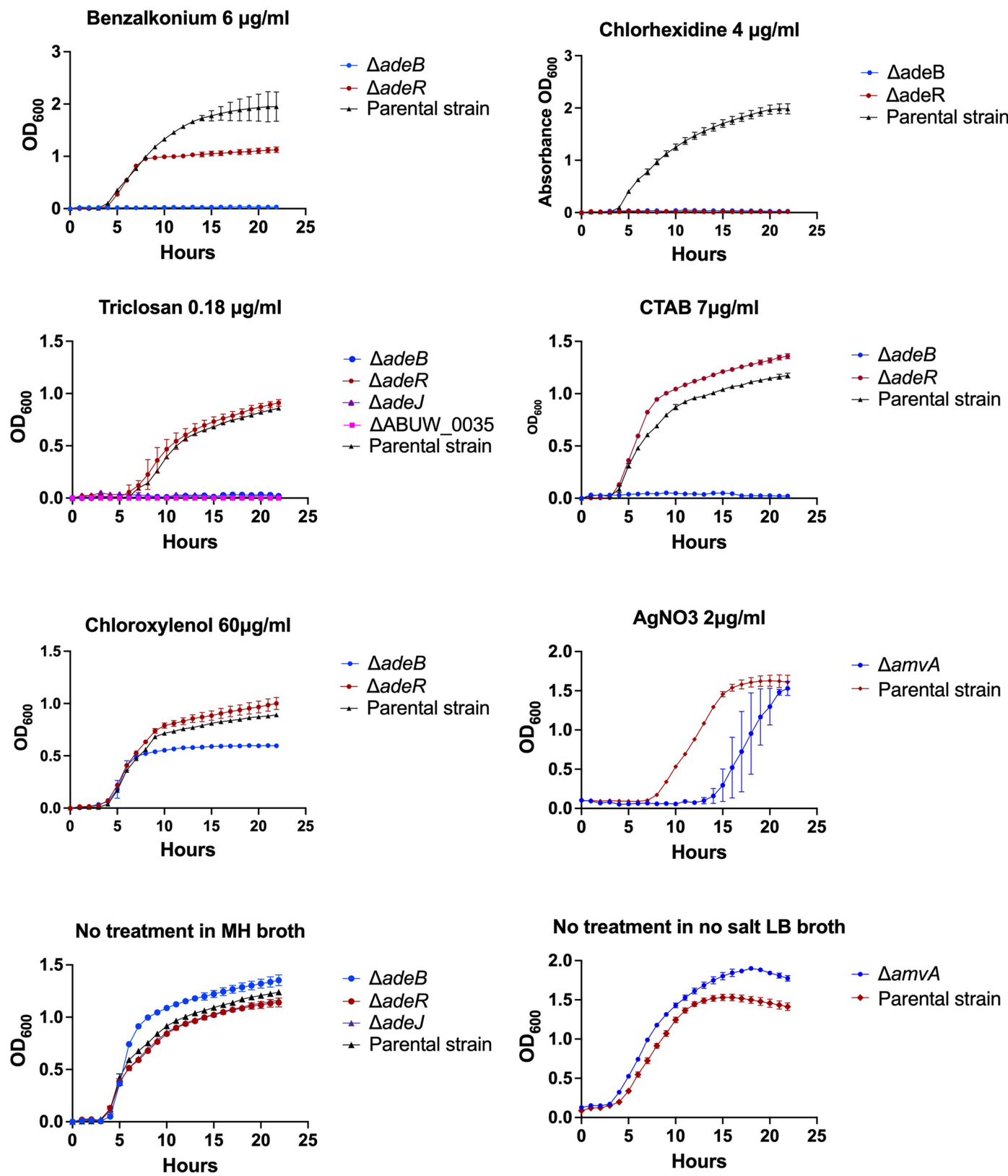
Extended Data Fig. 1 | TraDIS data validation. The growth curves of an individual transposon mutant were compared to the parental strain *A. baumannii* AB5075, with or without biocide treatment. The data are presented as mean values +/- standard deviation, from three independent biological replicates. The data was processed and plotted by Graph Pad Prism version 10.0.0 (131).



Extended Data Fig. 2 | See next page for caption.

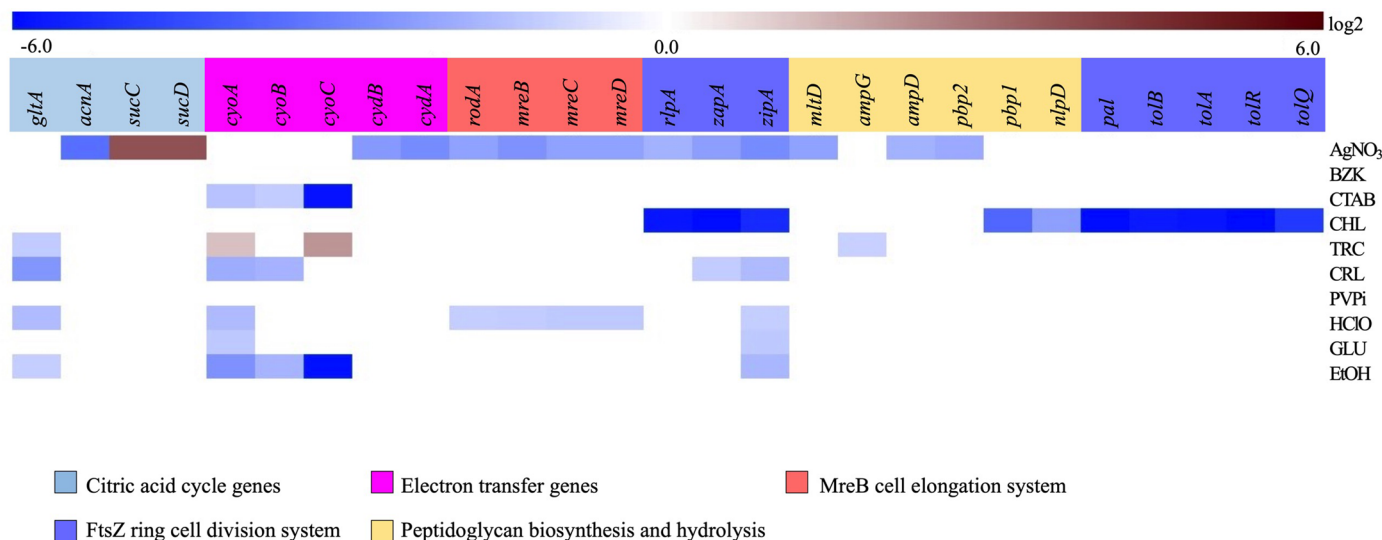
Extended Data Fig. 2 | Comparisons of biocide tolerance phenotype among different transposon mutants of the same gene. The transposon mutants of five genes, that showed changes in transposon insertion reads in the libraries treated by biocides, were chosen to be tested through growth curve assays. Two unique Tn5 transposon mutants of each of the five genes were tested. The data

are presented as mean values +/- standard deviation, from three independent biological replicates. The TraDIS results and transposon insertion sites of the mutants of choice are presented in Extended Data Table 3. The data was processed and plotted by Graph Pad Prism version 10.0.0 (131).

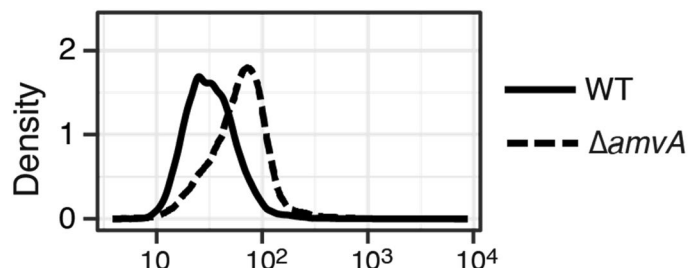


Extended Data Fig. 3 | Validation of drug efflux pump's role in biocide resistance. Growth curves of an individual transposon mutant of an efflux gene or the transcriptional regulator of an efflux gene were compared to the parental strain *A. baumannii* AB5075, with or without biocide treatment. The data are

presented as mean values +/- standard deviation, from three independent biological replicates. The data was processed and plotted by Graph Pad Prism 10.0.0 (131).

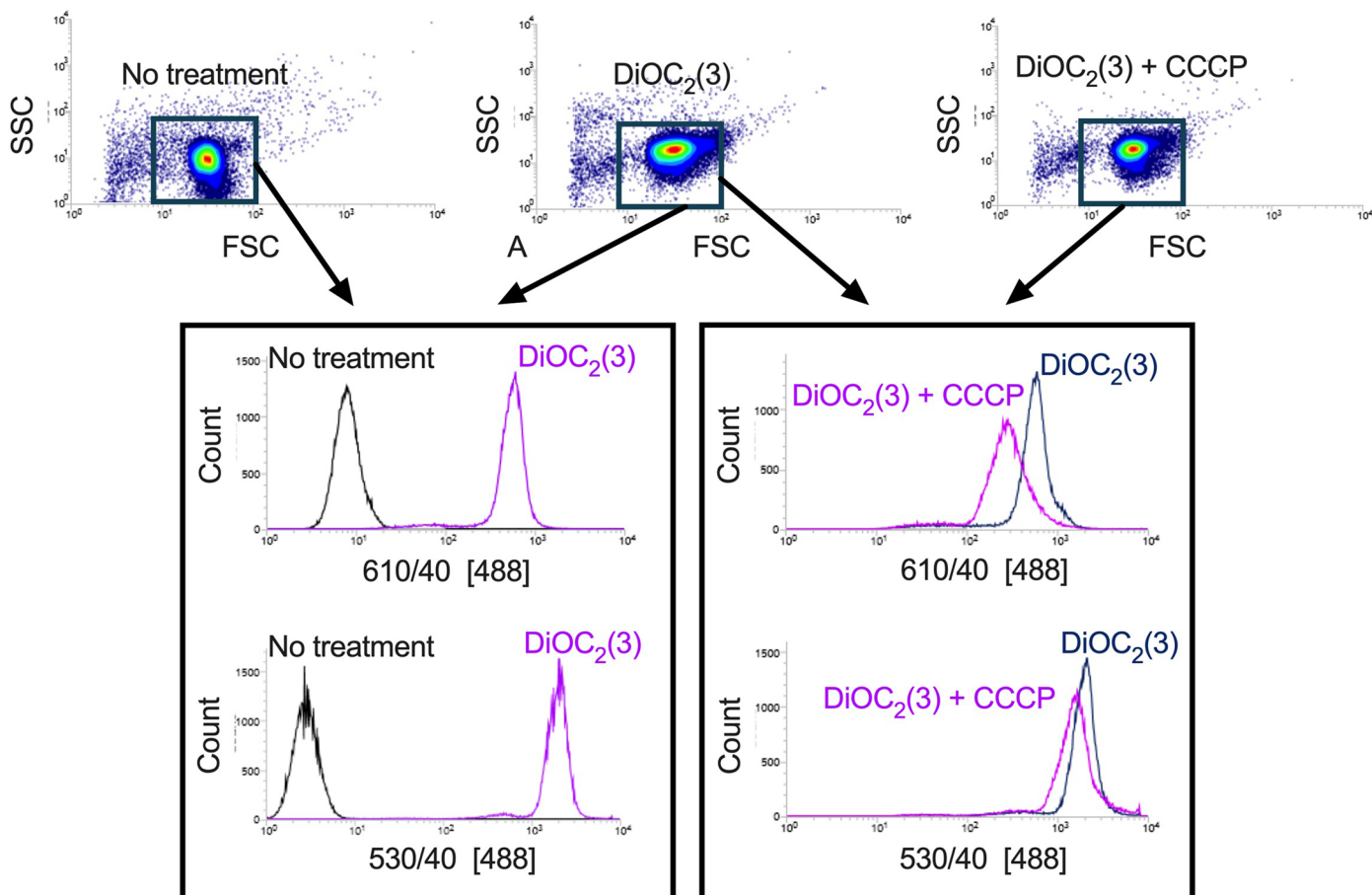


Extended Data Fig. 4 | TCA cycle, electron transfer and cell division. The heatmap represents transposon insertion read fold change of each gene, which is colour coded with darker blue indicating higher decrease in Tn5 insertion read coverage and darker red higher increase. The genes are grouped by cellular pathways, with colour scheme underneath.



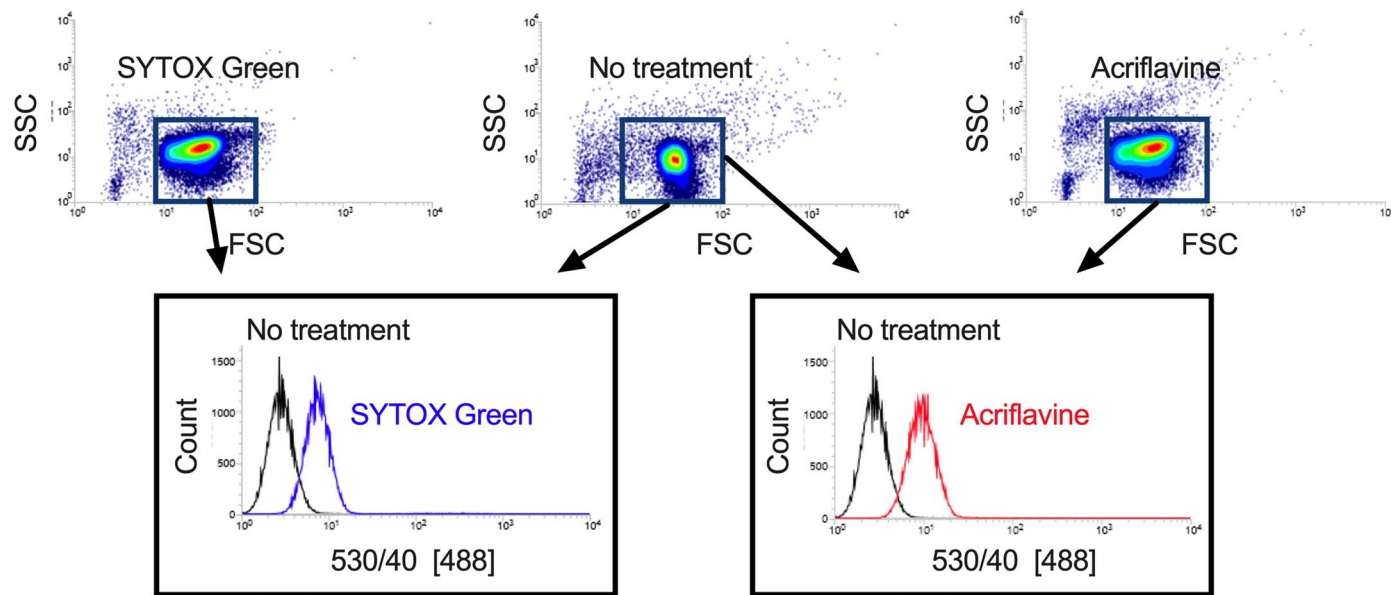
Extended Data Fig. 5 | The transposon mutant of $\Delta amvA$ derived from *A. baumannii* AB5075 accumulates more acriflavine than the parental strain.
The difference of acriflavine accumulation between $\Delta amvA$ and the parental strain were measured through flow cytometry (BD Influx™ Cell Sorter). Each

curve shows the fluorescence intensity for 50,000 cells. The cell populations show fluorescence profiles based on the concentration of acriflavine in the cell cytoplasm.



Extended Data Fig. 6 | Flow cytometry gating and control in membrane potential ($\text{DiOC}_2(3)$) assays. For each culture, a tight single population was detected and gated, as shown in the three dot plots in the top panel. Because we were measuring the membrane potential of the whole cell population, we gated the single tight population (>85% of the total event) and recorded the total population for follow-up analysis. The dot plots from the top left to the top right are the cells with no treatment, the cells with $\text{DiOC}_2(3)$ treatment only, and the cells with $\text{DiOC}_2(3)$ and CCCP treatments, respectively. CCCP is a proton ionophore and a positive control for inducing dissipation of membrane potential in this study. $\text{DiOC}_2(3)$ is excitable by blue laser (488 nm) and emit green (530/40) and red (610/40) light. The ratio of $\text{DiOC}_2(3)$ red/green fluorescence is positively

correlated to cell membrane potential. As shown in the bottom left panel, the cells without $\text{DiOC}_2(3)$ treatment had a lot lower fluorescence signal than the cells that was treated by $\text{DiOC}_2(3)$. This served as a background control that the fluorescence signals from the membrane potential assays (main text Fig. 3) are from intracellular $\text{DiOC}_2(3)$, rather than from cell auto fluorescence. As shown in the bottom right panel, CCCP induced a larger drop in red fluorescence than in green fluorescence, which resulted to a decrease in the ratio of red/green fluorescence (please also refer to Fig. 3 in the main text), indicating a drop in cell membrane potential. This indicated that $\text{DiOC}_2(3)$ is suitable for measuring membrane potential in *A. baumannii* via BD InfluxTM Cell Sorter. The dot plots and histograms were generated by BD InfluxTM Cell Sorter Software.



Extended Data Fig. 7 | Flow cytometry gating and control in SYTOX Green and acriflavine assays. The gating strategy and rationale in these assays are similar to the membrane potential assays. We were measuring and comparing the intracellular fluorescent dye concentration of the whole cell population, so we gated the tight single population, as shown in the three dot plots in the top panel. Both SYTOX Green and acriflavine can be excited by blue laser (488 nm) and emit green light (530/40 nm). The bottom left panel shows that the cells treated

by SYTOX Green emitted stronger green light than the cells without treatment, and the same for acriflavine in the bottom right panel. This guaranteed that the fluorescent events obtained in Fig. 4 in the main text were from cells containing either SYTOX Green or acriflavine and the fluorescence shifts were positively correlative to the intracellular concentration difference of either of the fluorescent dyes. The dot plots and histograms were generated by BD Influx™ Cell Sorter Software.

Extended Data Table 1 | Current knowledge of antibacterial actions and resistance mechanisms of the biocides tested in this study and a summary of TraDIS assay outcomes

Biocide (abbreviation)	Examples of clinical application	Proposed antibacterial action	Resistance mechanisms (resistance genes previously identified in <i>A. baumannii</i>)	Tn5 insertion read change	
				Genes > 2-fold increase	Genes > 2-fold decrease
Silver nitrate (AgNO_3)	Silver impregnated nylon cloth as wound dressing, Ag coated catheters	Inactivation of proteins containing exposed thiol groups and Fe-S clusters, inhibition of DNA synthesis	Efflux, silver efflux system periplasmic chaperone, cation/copper transporter	100	120
Benzalkonium (BZK)	Preoperative skin disinfection, hard-surface disinfection	Cell envelope disruption	Efflux (<i>abeS</i> , <i>adeABC</i> , <i>adelJK</i> , <i>amvA</i>)	7	45
Cetyltrimethylammonium bromide (CTAB)	Preoperative skin disinfection, cosmetics additive	Cell envelope disruption	Efflux (<i>abeS</i>)	35	42
Chlorhexidine (CHL)	Pharmaceutical preservative, skin, hand, and surgical disinfections	Phospholipid bilayer damage and unknown intracellular targets	Efflux (<i>aceI</i> , <i>abeS</i> , <i>adeABC</i> , <i>adelJK</i> , <i>amvA</i>), unidentified chlorhexidine-degrading enzyme	68	34
Triclosan (TRC)	Antiseptic soap, hand rinses, dental hygiene	Inhibits the FabI enoyl-acyl carrier protein reductase and blocks fatty acid biosynthesis	Efflux (<i>abeM</i> , <i>adeABC</i>), mutations on enoyl-(acyl-carrier-protein) reductase <i>FabI</i> (<i>fabI</i>), expression of expression of alternative enoyl reductase <i>FabK</i> , <i>FabL</i> or <i>FabV</i>	24	57
Chloroxylenol (CRL)	Surgical hand scrubs and other hand-washing products	Probable cell membrane destabilization	Efflux (A1S_2795 and ABAYE_0913 MFS family, A1S_1535 ABC family)	13	44
Polyvidone iodine (PVPi)	First aid and treatments for skin infection and wounds	Probable binding to key proteins with exposed cysteine and methionine residues, nucleotides, and fatty acids	None identified	9	3
Sodium hypochlorite (NaOCl)	Hard-surface disinfection, disinfection of blood spillages	DNA damage and inhibition of DNA biosynthesis	Glutathione, antioxidant against NaOCl	14	34
Glutaraldehyde (GLU)	Endoscopes and surgical equipment disinfection	Probable cell envelope disruption, inhibition of DNA, RNA, and protein synthesis	None identified	11	17
Ethanol (EtOH)	Hand sanitising	Probable disruption of phospholipid bilayer and cell lysis	Cell membrane alteration	13	18

References: [914–16, 40, 43, 44, 60–67](#)

Extended Data Table 2 | Biocide MIC values and their concentrations used in this study

Compound	MIC ($\mu\text{g/ml}$) ¹		TraDIS assay concentration ($\mu\text{g/ml}$)	Biocide concentration in membrane potential assay, acriflavine assays ² , and SYTOX TM Green assays ³ ($\mu\text{g/ml}$)	ATCC17978 time-kill curve assay ($\mu\text{g/ml}$)	Assay media
	BAL062	ATCC17978				
Triclosan (irgasan)	0.72	0.72	0.18	0.18	0.18	0.14% DMSO in MH
Chloroxylenol	240	240	60	60	N/A	0.14% DMSO in MH
Silver nitrate	24	8	6	6	N/A	LB without NaCl
Absolute ethanol	8%	12%	2%	2%	4%	MH
Sodium hypochlorite	0.24%	0.24%	0.06%	0.06%	N/A	MH
Glutaraldehyde	1800	1200	450	450	N/A	MH
Polyvidone iodine	4000	2000	1000	1000	600	MH
Chlorhexidine diacetate	20	16	5	5	2.5	MH
Benzalkonium chloride	16	16	4	4	4	MH
Cetyltrimethylammonium bromide	28	28	7	7	7	MH
CCCP (carbonyl cyanide m-chlorophenyl hydrazone)	N/A	N/A	N/A	5	5	MH
Gentamicin	10,000	2	N/A	N/A	4	MH
Amikacin	2000	3.5	N/A	N/A	7.5	MH
Tigecycline	2	2	N/A	N/A	7.5	MH
Ciprofloxacin	250	0.5	N/A	N/A	1	MH
Imipenem	80	1.25	N/A	N/A	2.5	MH
Colistin	5	1.5	N/A	N/A	3.5	MH

Footnote: 1. The antimicrobial MIC values are for *A. baumannii* BAL062 and ATCC17978, respectively. 2. Acriflavine at 3 $\mu\text{g/ml}$, equal to 1/32 MIC in *A. baumannii* BAL062, was used for flow cytometry assays in *A. baumannii* BAL062. 3. SYTOXTM Green at 1 μM was used for cell membrane permeability assays through flow cytometry in *A. baumannii* BAL062.

Extended Data Table 3 | Transposon mutants of *A. baumannii* AB5075 selected for growth curve assays in this study

Locus tag	Gene name or function	Transposon insertion site/gene length	Tn5 insertion read change (log2) ¹								
			AgNO3	TRC	BZK	CTAB	CHL	CRL	NaOCl	Glu	EtOH
ABUW_0622	<i>trpA</i>	433/804	ns	ns	ns	-1.99	ns	-1.41	-2.12	-1.45	-1.89
ABUW_0867	<i>gltA</i>	563/1275	ns	-1.23	ns	-0.87	ns	-2.56	-1.58	ns	-1.15
ABUW_0466	Ribonuclease I	320/633	ns	-1.66	-1.54	-1.97	ns	-1.12	ns	-1.10	-0.77
ABUW_1975	<i>adeB</i>	150/3108	ns	-2.99	-6.85	-1.15	-6.42	-1.02	ns	ns	ns
ABUW_1973	<i>adeR</i>	195/744	ns	ns	-2.92	ns	-4.74	ns	ns	ns	ns
ABUW_0843	<i>adeJ-1</i>	1711/3177		-2.14	-1.12	ns	-4.16	-2.55	ns	ns	ns
	<i>adeJ-2</i>	956/3177									
ABUW_0035	RND efflux transporter	2427/3126	ns	-2.87	ns						
ABUW_1679	<i>amvA-1</i>	495/1479	-4.28	ns	-0.64	ns	-6.73	ns	ns	ns	ns
	<i>amvA-2</i>	785/1497									
ABUW_3846	<i>dsbA-1</i>	184/618	-0.86	-2.59	-0.97	-1.09	ns	-0.98	ns	ns	ns
	<i>dsbA-2</i>	336/618									
ABUW_0953	<i>lysA-1</i>	390/1251	-0.79	0.58	ns	ns	ns	-0.87	-1.06	ns	-2.83
	<i>lysA-2</i>	721/1251									
ABUW_0999	<i>rvuB-1</i>	267/1005	ns	ns	ns	ns	ns	ns	-1.09	-2.08	ns
	<i>rvuB-2</i>	350/1005									
ABUW_2825	<i>pyrC</i>	337/1035	5.17	1.19	ns	0.58	ns	0.86	ns	ns	ns
ABUW_3448	<i>lpsB</i>	414/1101	-1.13	-2.35	1.00	ns	ns	-1.29	ns	ns	ns

Footnote: 1. The fold change values with bold font represent the biocide sensitivity of the respective mutants were selected for growth curve assays or MIC assays (Fig. 1b, S1, S2 and S3). 2. "ns" means not significant.

Reporting Summary

Nature Portfolio wishes to improve the reproducibility of the work that we publish. This form provides structure for consistency and transparency in reporting. For further information on Nature Portfolio policies, see our [Editorial Policies](#) and the [Editorial Policy Checklist](#).

Statistics

For all statistical analyses, confirm that the following items are present in the figure legend, table legend, main text, or Methods section.

n/a Confirmed

- The exact sample size (n) for each experimental group/condition, given as a discrete number and unit of measurement
- A statement on whether measurements were taken from distinct samples or whether the same sample was measured repeatedly
- The statistical test(s) used AND whether they are one- or two-sided
Only common tests should be described solely by name; describe more complex techniques in the Methods section.
- A description of all covariates tested
- A description of any assumptions or corrections, such as tests of normality and adjustment for multiple comparisons
- A full description of the statistical parameters including central tendency (e.g. means) or other basic estimates (e.g. regression coefficient) AND variation (e.g. standard deviation) or associated estimates of uncertainty (e.g. confidence intervals)
- For null hypothesis testing, the test statistic (e.g. F , t , r) with confidence intervals, effect sizes, degrees of freedom and P value noted
Give P values as exact values whenever suitable.
- For Bayesian analysis, information on the choice of priors and Markov chain Monte Carlo settings
- For hierarchical and complex designs, identification of the appropriate level for tests and full reporting of outcomes
- Estimates of effect sizes (e.g. Cohen's d , Pearson's r), indicating how they were calculated

Our web collection on [statistics for biologists](#) contains articles on many of the points above.

Software and code

Policy information about [availability of computer code](#)

Data collection	Tranposon insertion site reads were mapped by Bio-Tradis (available in GitHub). Flow cytometry data were collected through BD Influx Software. Growth curve data were collected through "Reader Control" and "MARS Data Analysis Sofware 3.20 R2". qPCR data were collected through ROCHE "LightCycler 480 Software release 1.5.1.62 SP2".
Data analysis	Time kill curve data and flow cytometry data were analyzed through R with custom codes. The data of growth curves, qPCR, and membrane potential are analyzed by Graph Pad Prism 10.0.0 (131)..

For manuscripts utilizing custom algorithms or software that are central to the research but not yet described in published literature, software must be made available to editors and reviewers. We strongly encourage code deposition in a community repository (e.g. GitHub). See the Nature Portfolio [guidelines for submitting code & software](#) for further information.

Data

Policy information about [availability of data](#)

All manuscripts must include a [data availability statement](#). This statement should provide the following information, where applicable:

- Accession codes, unique identifiers, or web links for publicly available datasets
- A description of any restrictions on data availability
- For clinical datasets or third party data, please ensure that the statement adheres to our [policy](#)

TraDIS sequencing data was deposited in the European Nucleotide Database under project number PRJEB8707

Human research participants

Policy information about [studies involving human research participants and Sex and Gender in Research](#).

Reporting on sex and gender

Not applicable

Population characteristics

Not applicable

Recruitment

Not applicable

Ethics oversight

Not applicable

Note that full information on the approval of the study protocol must also be provided in the manuscript.

Field-specific reporting

Please select the one below that is the best fit for your research. If you are not sure, read the appropriate sections before making your selection.

Life sciences

Behavioural & social sciences

Ecological, evolutionary & environmental sciences

For a reference copy of the document with all sections, see nature.com/documents/nr-reporting-summary-flat.pdf

Life sciences study design

All studies must disclose on these points even when the disclosure is negative.

Sample size

Three biological replicates were included in all the experiments in this study, except for TraDIS assays. TraDIS assays used two biological replicates for each condition. This is because each TraDIS biological replicate contained more than 100k unique transposon insertion mutants, which itself will provide very high statistical confidence.

Data exclusions

No data was excluded.

Replication

Three biological replicates were included in all of the experiments in this study, except for TraDIS assays. There were some variations among the biological replicate data, but the differences among the experimental groups are statistically significant. Two independent TraDIS biological replicates were performed for each condition. Both of the TraDIS replicates of each condition produced data of high statistical confidence.

Randomization

The biological replicates were derived from individual colonies that were randomly picked from an agar plate.

Blinding

Blinding was not relevant to this study. The key criteria in determining whether the observations were reproducible is that different batch of cells can produce consistent data/results on different days, which do not need blinding.

Reporting for specific materials, systems and methods

We require information from authors about some types of materials, experimental systems and methods used in many studies. Here, indicate whether each material, system or method listed is relevant to your study. If you are not sure if a list item applies to your research, read the appropriate section before selecting a response.

Materials & experimental systems

n/a	Involved in the study
<input checked="" type="checkbox"/>	<input type="checkbox"/> Antibodies
<input checked="" type="checkbox"/>	<input type="checkbox"/> Eukaryotic cell lines
<input checked="" type="checkbox"/>	<input type="checkbox"/> Palaeontology and archaeology
<input checked="" type="checkbox"/>	<input type="checkbox"/> Animals and other organisms
<input checked="" type="checkbox"/>	<input type="checkbox"/> Clinical data
<input checked="" type="checkbox"/>	<input type="checkbox"/> Dual use research of concern

Methods

n/a	Involved in the study
<input checked="" type="checkbox"/>	<input type="checkbox"/> ChIP-seq
<input type="checkbox"/>	<input checked="" type="checkbox"/> Flow cytometry
<input checked="" type="checkbox"/>	<input type="checkbox"/> MRI-based neuroimaging

Flow Cytometry

Plots

Confirm that:

- The axis labels state the marker and fluorochrome used (e.g. CD4-FITC).
- The axis scales are clearly visible. Include numbers along axes only for bottom left plot of group (a 'group' is an analysis of identical markers).
- All plots are contour plots with outliers or pseudocolor plots.
- A numerical value for number of cells or percentage (with statistics) is provided.

Methodology

Sample preparation

Multiple colonies were picked from an agar plate. The colonies were inoculated in MH broth and grew overnight at 37°C and with shaking at 200rpm. The overnight cultures were diluted 1/100 in fresh MH broth and subcultured at the same condition till OD₆₀₀ reached 0.4. The subcultures were treated by different conditions for 2-5 minutes at 37°C with shaking at 200rpm. After this the subcultures were diluted to density around 10⁶ cell per ml before flow cytometry. More information please refer to the "Methods and Materials" section in the article.

Instrument

BD Influx

Software

BD Influx Software

Cell population abundance

Pure bacterial cultures were analyzed. The culture density was around 10⁶ cells per ml.

Gating strategy

We gated 50,000 cells based on their FSC and SSC to exclude the minority elongated cells and cell debris, and recorded all the events for the final data analysis. Please refer Extended Data Figure S6 and S7 for more detail.

- Tick this box to confirm that a figure exemplifying the gating strategy is provided in the Supplementary Information.